

See discussions, stats, and author profiles for this publication at: <https://www.researchgate.net/publication/46158947>

# ChemInform Abstract: Advances in Selective Conversions by Heterogeneous Photocatalysis

ARTICLE *in* CHEMICAL COMMUNICATIONS · OCTOBER 2010

Impact Factor: 6.83 · DOI: 10.1039/c0cc02087g · Source: PubMed

CITATIONS

155

READS

132

7 AUTHORS, INCLUDING:



**Giovanni Palmisano**

Masdar Institute of Science and Technology

76 PUBLICATIONS 2,109 CITATIONS

SEE PROFILE



**Elisa Isabel Garcia Lopez**

Università degli Studi di Palermo

50 PUBLICATIONS 1,654 CITATIONS

SEE PROFILE



**Sedat Yurdakal**

Afyon Kocatepe University

37 PUBLICATIONS 1,108 CITATIONS

SEE PROFILE



**Leonardo Palmisano**

Università degli Studi di Palermo

257 PUBLICATIONS 10,416 CITATIONS

SEE PROFILE

# Advances in selective conversions by heterogeneous photocatalysis

Giovanni Palmisano,<sup>a</sup> Elisa García-López,<sup>a</sup> Giuseppe Marci,<sup>a</sup> Vittorio Loddo,<sup>a</sup> Sedat Yurdakal,<sup>ab</sup> Vincenzo Augugliaro<sup>\*a</sup> and Leonardo Palmisano<sup>\*a</sup>

Received 25th June 2010, Accepted 4th August 2010

DOI: 10.1039/c0cc02087g

Selective photocatalytic conversions are offering an alternative green route for replacing environmentally hazardous processes with safe and energy efficient routes. This paper reports the most recent advances in the application of heterogeneous photocatalysis to synthesize valuable compounds by selective oxidation and reduction.

Heterogeneous photocatalysis is an advanced oxidation process which is the subject of a huge amount of studies related to environment recovery, such as air cleaning and water purification, in which organic and inorganic pollutants are totally degraded to innocuous substances over mainly TiO<sub>2</sub> photocatalysts.<sup>1</sup> Only recently studies have been conducted on the application of photocatalysis for product synthesis by selective oxidation and reduction.<sup>2</sup> These studies demonstrate that high selectivities can be obtained in photo-oxidation and photoreduction processes as compared with conventional ones. As far as the irradiation sources are concerned, medium or high pressure Hg lamps have been often used, together with visible light lamps and solar radiation simulators. Literature studies using only sunlight are not very frequent because the reproducibility of the measurements is in this case a hard task. Nevertheless most of the syntheses reported can be virtually carried out under sunlight. The present paper illustrates the most recent advances in the application of heterogeneous photocatalysis to selective conversions.

<sup>a</sup> "Schiavello-Grillone" Photocatalysis Group – Dipartimento di Ingegneria Chimica dei Processi e dei Materiali – Università degli Studi di Palermo, Viale delle Scienze, 90128 Palermo, Italy.  
E-mail: augugliaro@dicpm.unipa.it, palmisano@dicpm.unipa.it;  
Fax: +39 091 7025020; Tel: +39 091 23863746

<sup>b</sup> Kimya Bölümü, Fen-Edebiyat Fakültesi, Afyon Kocatepe Üniversitesi, Ahmet Necdet Sezer Kampüsü, 03100 Afyon, Turkey

## 1. Oxidation

Oxidation processes play an important role in the production of a wide range of chemicals. Many of them as aldehydes, ketones or epoxides, are precursors in the synthesis of added value organic compounds as drugs, vitamins or fragrances. Notwithstanding their importance, very few green chemistry oxidation processes obtain these substances. In this framework, photocatalytic method can be cogitated as a possible alternative approach to traditional industrial oxidation processes which need stringent reaction conditions and oxidants as mineral acids, chromates, permanganate, hydrogen peroxide, *etc.* questionable from the points of view of toxicity and corrosiveness.

### 1.1 Partial oxidation of alcohols

Methanol, produced from natural gas, coal and biomass is an attractive starting material to obtain various important industrial chemicals. Photocatalytic oxidation of methanol in a continuous gas–solid reactor in the presence of commercial anatase TiO<sub>2</sub> particles<sup>3</sup> has yielded different products such as methyl formate, one of the precursors of formamide, ethyl-ene glycol, formic acid and acetic acid. Methyl formate was obtained at room temperature with a selectivity of 87–91%, whereas formaldehyde, CO and CO<sub>2</sub> were detected as minor products. The Authors claim that contact time of the gas mixture with TiO<sub>2</sub> is one of the key factors to obtain a good selectivity, avoiding the deep oxidation of the desired product;



Giovanni Palmisano

Giovanni Palmisano got his PhD degree in Chemical and Materials Engineering at the University of Palermo in 2009. He currently works on photocatalysis and dye solar cells. He has co-authored ca. 35 research papers on these fields and in particular on advanced oxidation processes for environment remediation and for organic synthesis. He is also co-author of the book "Flexible solar cells" published by Wiley VCH.



Elisa García-López

Elisa García-López received her BS in Chemistry at the Universidad Autónoma de Madrid (Spain) and her PhD degree at the University of Palermo. She was a post-doctoral researcher at the Meisei University in Tokyo and she is currently Assistant Professor in Chemistry at the University of Palermo. The main focus of her work is heterogeneous photocatalysis.

in fact at low flow rate the selectivity decreases by increasing the CO<sub>2</sub> amount. Another parameter influencing the selectivity is the reaction temperature: at 523 K the conversion is three times higher than at room temperature but the selectivity decreases. FTIR spectra of the adsorbed species before and after the irradiation suggest that the oxidation reaction proceeds through the dimerization of the formaldehyde produced during the reaction.

Selective and efficient photocatalytic oxidation of alcohols to their corresponding aldehydes and ketones in liquid–solid regime is one of the most important reactions both in industrial and laboratory synthesis. The detailed mechanism for this selective oxidation is still unclear due to the non selectivity of OH radical attack. Moreover, the slow reaction rates still remain one of the obstacles in the application of these selective photocatalytic reactions.

Zhang *et al.*<sup>4</sup> have studied the mechanism of the photocatalytically oxidative transformation of alcohols performed in benzotrifluoride (BTF) by using bare TiO<sub>2</sub> anatase. They have found an oxygen transfer from molecular O<sub>2</sub> to the

alcohol. The oxygen atom of the alcohol is completely replaced by one of the oxygen atoms of the dioxygen molecule, *i.e.* the process occurs by the selective cleavage of the C–OH bond with the concomitant formation of a C=O bond to form the final product, where the O comes from O<sub>2</sub>.

The mechanism proposed by the Authors (Fig. 1) is the following one. The alcohol molecule is adsorbed onto the surface of TiO<sub>2</sub> by a deprotonation process, hence it reacts with the photogenerated hole on the TiO<sub>2</sub> surface forming a carbon radical whereas the electron transforms Ti(IV) in Ti(III). Both the carbon radical and Ti(III) easily react with O<sub>2</sub> and a

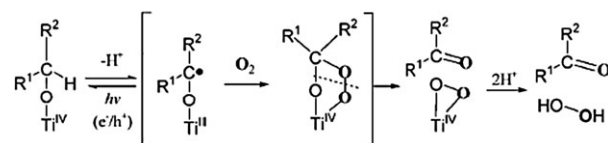


**Fig. 1** Proposed mechanism<sup>4</sup> in the photocatalytic partial oxidation of alcohols in BTF.



**Giuseppe Marci**

*Giuseppe Marci studied Chemical Engineering and received his PhD in Chemical Engineering in 1997. He is Assistant Professor in Chemistry at the University of Palermo where he teaches Chemistry and develops his work in the fields of Photocatalysis and Materials Chemistry. He is the co-author of 79 articles and 141 papers in proceedings of congress.*



**Vittorio Loddo**

*Vittorio Loddo received the degree in Chemical Engineering from the University of Palermo in 1993 and the PhD degree in Chemical Engineering from the “Federico II” University of Naples in 1998. From August 2000 he is Assistant Professor of Transport Phenomena at the University of Palermo. In the course of his scientific activity, he has contributed to the following fields: chemical kinetics of heterogeneous photocatalytic systems; modelling of heterogeneous photoreactors, radiation field modelling in absorbing–reacting media, advanced oxidation processes for environment remediation.*



**Sedat Yurdakal**

*preparation of new materials adsorption determination.*

*Sedat Yurdakal received his high degree in Chemistry in 2000 at the University of Anadolu, Eskişehir, Turkey. He started to work as a research assistant at the University of Afyon Kocatepe in 2001. He performed his PhD Thesis work at the University of Palermo and University of Anadolu from 2003 to 2010. He has published several papers in international journals and books on selective photocatalytic oxidations in water, containing TiO<sub>2</sub> and photo-*

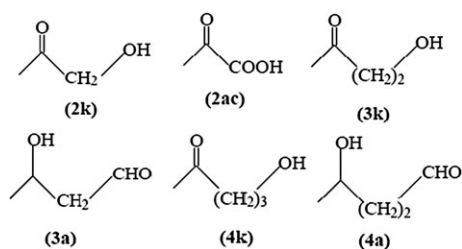


**Vincenzo Augugliaro**

*Vincenzo Augugliaro is Full Professor of Transport Phenomena at the University of Palermo. His investigation has concerned the fields of: chemical absorption kinetics, chemical kinetics of heterogeneous photocatalytic systems, modelling of heterogeneous photoreactors, radiation field modelling in absorbing–reacting media, advanced oxidation processes for environment remediation and for organic synthesis. He is author of hundreds of papers published in international journals and books and oral or poster communications in National and International Conferences.*

Ti peroxide intermediate is formed. The cleavage of this species gives rise to carbonylic species, coming from the partial oxidation of the alcohol. The same Authors carried out the same reaction in the presence of Brønsted acids and they observed an enhancement of both reaction rate and selectivity.<sup>5</sup> The effect is related to the decomposition of the relatively stable side-on peroxide intermediate by the protons of the Brønsted acids, which can clean the catalytic Ti-OH<sub>2</sub> sites. This finding opens a new path to obtain high selectivity and conversion by TiO<sub>2</sub> photocatalysis.

It is accepted that adsorption of the alcohol onto the photocatalysts surface is a mandatory requirement for its oxidation. Indeed, some Authors propose the dissociative adsorption forming an alkoxide intermediate. There is an agreement in the literature about the relevance of this point. For instance, it has been demonstrated that primary alcohols, as 1,*n*-diols, show an increased reactivity with respect to secondary ones due to the site selective adsorption. Molinari *et al.*<sup>6</sup> report the partial photooxidation of diols as 1,3-butanediol and 1,4-pentanediol and *vic*-diols as 1,2 propanediol by using TiO<sub>2</sub> in dichloromethane. CO<sub>2</sub> is not revealed as a reaction product but for each 1,*n*-diol the main reaction products are two hydroxy-carbonyl compounds. 1,2-propanediol gives rise mainly to hydroxyacetone (2k) with a selectivity of 90% with traces of pyruvic acid (2ac), 1,3-butanediol to 3-hydroxybutyraldehyde (3a) and 4-hydroxy-2-butanone (3k) and 1,4-pentanediol to 4-hydroxypentanal (4a) with a selectivity of 75% and 3-acetyl 1-propanol (4k). Table 1 reports qualitatively and quantitatively these results.



**Leonardo Palmisano**

*Leonardo Palmisano is Full Professor of Chemistry at the University of Palermo. His main field of interest is heterogeneous photocatalysis and he is author of hundreds of papers published in international journals and books and oral or poster communications in National and International Conferences. He has been invited as Visiting Researcher (Bradford University, UK), Visiting Professor (Hokkaido University, Japan) or Lecturer*

*in many Universities all over the world. He is also the co-author of the didactic book "Fondamenti di Chimica" published in Italy by Edises and in Spain by Ariel Ciencia.*

**Table 1** Carbonyl compounds distribution in the photocatalytic oxidation of 1,*n*-diols by TiO<sub>2</sub>.<sup>6</sup> *n<sub>k</sub>* represents the ketone, *n<sub>a</sub>* the aldehyde and *n<sub>ac</sub>* the acid

Diol	<i>n<sub>k</sub></i> /μmol	<i>n<sub>a</sub></i> /μmol	<i>n<sub>ac</sub></i> /μmol	Aldehyde/ketone
<i>n</i> = 2	0.5	Not formed	0.07	0
<i>n</i> = 3	2.4	2.7	Not formed	1.1
<i>n</i> = 4	1.9	6.5	Not formed	3.4

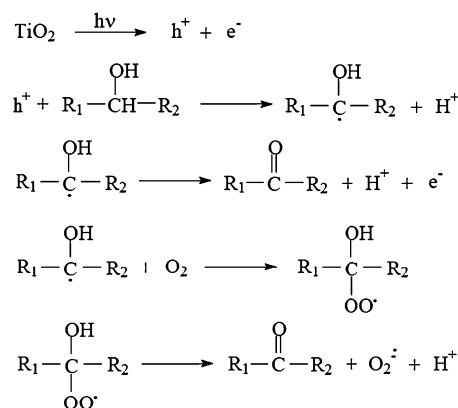


**Fig. 2** Mechanism for the direct oxidation of alcohols.<sup>6</sup>

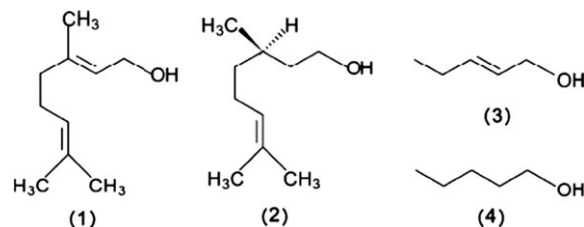


**Fig. 3** Allylic alcohols photocatalytically oxidised.<sup>7</sup>

Besides the oxidation mechanism of the alkoxide by means of the OH radicals photogenerated by hole trapping, the possibility of direct oxidation of the adsorbed alkoxide by the holes is also invoked<sup>6</sup> (Fig. 2).

Molinari *et al.*<sup>7</sup> have investigated also the photocatalytic partial oxidation of some allylic alcohols (shown in Fig. 3) as geraniol (1) and *trans*-2-penten-1-ol (3) along with primary alcohols as citronellol (2) and 1-pentanol (4).

The study of the reaction mechanism by EPR revealed that not only the photogenerated hole but also the OH radical are involved in the oxidation of the substrate. In the absence of water the photocatalytic partial oxidation of geraniol produces only citral; however in the presence of water, OH radical can attack geraniol not selectively giving rise to the total and not selective degradation of the substrate. Moreover the Authors indicate that the presence of water inhibits the adsorption of geraniol and so it has a negative effect on the formation of citral abating the selectivity. Already a 2% of water increases significantly the polarity of the medium thus decreasing the adsorption of the substrate that competes with water for the adsorption sites.

As far as the two primary alcohols (geraniol and citronellol) are concerned, their great hydrophobic tails hinder the adsorption of these molecules in the presence of water that



displaces easily these substrates from the surface of the photocatalyst. On the contrary, 1-pentanol and *trans*-2-penten-1-ol are less influenced by the presence of water; consequently they are able to interact with the surface of the photocatalyst even when the surface is partially polar. Short alcohols such as methanol and 2-propanol<sup>8</sup> are degraded even in a water medium.

The photocatalytic oxidation of aromatic alcohols into the corresponding aldehydes proceeds also at high conversion and selectivity by using TiO<sub>2</sub> under oxygen atmosphere, in acetonitrile medium, according to Higashimoto *et al.*<sup>9</sup> The distinctiveness is that the reaction proceeds not only under UV, but also under visible irradiation due to the formation of surface complex species by the adsorbed aromatic alcohol. In order to clarify this point, the Authors carried out the reaction by using fluorinated TiO<sub>2</sub>, as reported by Minero *et al.*<sup>10</sup> They observed a dramatic decrease of photocatalytic activity under visible irradiation. This achievement obviously suggests a significant role played by the adsorption of the aromatic alcohol species on the surface of the solid involving the surface OH species.

Benzyl alcohol and some of its derivatives (*para*- structures) were transformed into the corresponding aldehydes with a conversion and selectivity of *ca.* 99% both under UV and visible irradiation. The only exception to this behaviour was the 4-hydroxybenzyl alcohol that was oxidized to 4-hydroxy benzaldehyde (selectivity of *ca.* 23% with a conversion of *ca.* 85%) along with some unidentified products.

The Authors claim that the OH groups of the TiO<sub>2</sub> surface react with the aromatic compound to form Ti–O–Ph species, exhibiting strong absorption in the visible region by ligand to metal charge transfer. This insight confirms the results reported by Choi *et al.*<sup>11</sup> which proposed a direct electron transfer from the surface-complexes to the conduction band of the TiO<sub>2</sub> upon absorbing visible light evidencing that visible light can induce reactions by substrate–surface complexation enabling the visible light absorption.

Fig. 4 summarizes the reaction pathway proposed by Higashimoto *et al.*<sup>9</sup> for the selective photocatalytic oxidation of benzyl alcohol in the presence of O<sub>2</sub> and TiO<sub>2</sub>. The surface

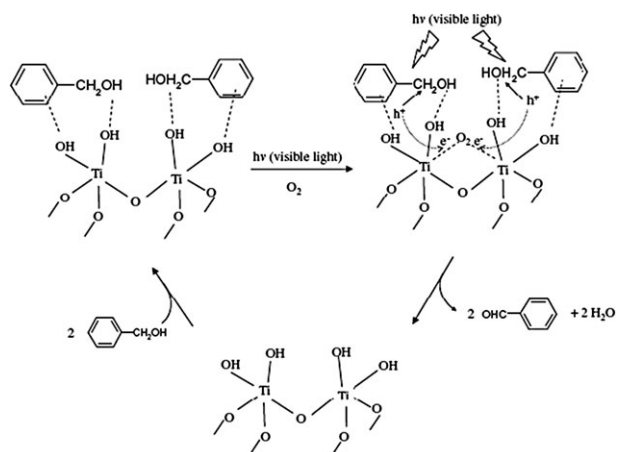


**Fig. 4** Proposed reaction mechanism for the photocatalytic oxidation of benzyl alcohol under visible light irradiation.<sup>9</sup>

complexes formed by the interaction of the alcohol group or the aromatic ring with the OH surface group are able to absorb in the visible region, hence the photoexcited complex undergoes a H abstraction in the CH<sub>2</sub>OH group by the photoproduct holes forming a water molecule. The organic radical also releases one electron to form benzaldehyde. At the same time the photoinduced electrons are trapped by the O<sub>2</sub> in the reacting medium.

The oxidation of some aromatic alcohols by using aqueous suspensions of home-prepared TiO<sub>2</sub> samples has been the object of a sound investigation<sup>12–14</sup> by our research group; the main findings obtained with methoxybenzyl alcohol (MBA) are summarized in the following. Partial oxidation occurs to 4-methoxybenzaldehyde (*p*-anisaldehyde, PAA) by all the home-prepared samples that showed selectivity far higher than those observed with commercial specimens. In all cases the photocatalytic oxidation of MBA proceeds through two parallel reaction routes effective from the start of irradiation: the first one determines the MBA partial oxidation to PAA while the second one eventually causes the MBA mineralization to CO<sub>2</sub> without the formation of volatile organic compounds. Selectivities as high as 74% with alcohol conversions up to 80% have been interestingly found by using some home-prepared TiO<sub>2</sub> samples obtained by low temperature treatments.<sup>15</sup>

Besides TiO<sub>2</sub>, other solid semiconductors or substances have been tested. Heteropoly acid solids (HPAs), also called polyoxometallates (POM), are ionic crystals consisting of large polyanions (primary structure) along with cations, water of crystallization and other molecules (secondary structure). They are used in solution as well as in the solid state as acid and oxidation catalysts.<sup>16</sup> POMs share photochemical characteristics with semiconductor photocatalysts; indeed, both classes of materials are constituted by d<sup>0</sup> transition metal and oxide ions and exhibit similar electronic characteristics (HOMO–LUMO transition for the POMs and band-gap transition for semiconductors). Hence, POMs not only are bifunctional acid–base and redox catalysts but also they can be activated by light. The irradiation in the UV-Vis region results in an oxygen to metal charge transfer excited state which is able to draw oxidation reactions. The photoexcited POM is then reduced but its regeneration is easily obtained by oxidation with the O<sub>2</sub> present in the reacting medium. POMs have been extensively used in photocatalytic reactions in homogeneous systems due to their solubility, particularly in water, however the heterogeneization of these inorganic salts can provide improvements in the photocatalytic features of the semiconductor.<sup>17</sup> Acidic or neutral substances such SiO<sub>2</sub>, activated carbon, or resins are suitable supports for HPAs whereas basic solids tend to decompose them by the hydrolysis of the heteropolyanion.

Farhadi *et al.*<sup>18a</sup> report the partial oxidation of benzylic alcohols using sol–gel silica-encapsulated H<sub>3</sub>PW<sub>12</sub>O<sub>40</sub> as a heterogeneous photocatalyst. They optimize the reaction conditions for the partial oxidation of 1-phenyl ethanol to acetophenone with yield of 84% within 2 h (Fig. 5).

Previously<sup>18b</sup> acetophenone had been obtained starting from cumene in liquid acetonitrile-oxygenated dispersions in the presence of TiO<sub>2</sub> catalyst irradiated by near UV light.

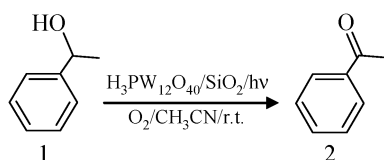


**Fig. 5** Photocatalytic oxidation of 1-phenyl ethanol<sup>18</sup> (1) to acetophenone (2) by using heterogeneized POM.

**Table 2** Photocatalytic oxidation of benzylic alcohols<sup>18</sup> with O<sub>2</sub> catalyzed by H<sub>3</sub>PW<sub>12</sub>O<sub>40</sub>/SiO<sub>2</sub>

Ar(CHOH)R → Ar(CO)R			
Ar	R	Irradiation time/h	Yield [%]
C <sub>6</sub> H <sub>5</sub>	H	2.5	75
<i>p</i> -MeC <sub>6</sub> H <sub>4</sub>	H	1	92
<i>o</i> -MeC <sub>6</sub> H <sub>4</sub>	H	1	90
<i>p</i> -ButC <sub>6</sub> H <sub>4</sub>	H	1.5	82
<i>p</i> -MeOC <sub>6</sub> H <sub>4</sub>	H	1.5	85
<i>o</i> -MeOC <sub>6</sub> H <sub>4</sub>	H	2	70
<i>p</i> -ClC <sub>6</sub> H <sub>4</sub>	H	1.5	80
<i>p</i> -BrC <sub>6</sub> H <sub>4</sub>	H	2	82
C <sub>6</sub> H <sub>5</sub>	CH <sub>3</sub>	2	84
<i>p</i> -MeC <sub>6</sub> H <sub>4</sub>	CH <sub>3</sub>	1	97
<i>p</i> -NO <sub>2</sub> C <sub>6</sub> H <sub>4</sub>	CH <sub>3</sub>	3	76
C <sub>6</sub> H <sub>5</sub>	C <sub>2</sub> H <sub>5</sub>	1.5	90
C <sub>6</sub> H <sub>5</sub>	C <sub>6</sub> H <sub>5</sub>	2	84
<i>p</i> -ClC <sub>6</sub> H <sub>4</sub>	C <sub>6</sub> H <sub>5</sub>	1.5	88
<i>p</i> -MeOC <sub>6</sub> H <sub>4</sub>	C <sub>6</sub> H <sub>5</sub>	1.25	90
<i>p</i> -NO <sub>2</sub> C <sub>6</sub> H <sub>4</sub>	C <sub>6</sub> H <sub>5</sub>	3	72
C <sub>6</sub> H <sub>5</sub>	-CH <sub>2</sub> OH	2	75

Table 2 reports the results in the photocatalytic partial oxidation of different aromatic alcohols. An ionic solvent can increase the conversion of *ca.* 5% in comparison to acetonitrile.<sup>19</sup>

By using POM/ZrO<sub>2</sub> nanocomposites, aliphatic alcohols have been also partially oxidized in good yields albeit after longer reaction times.<sup>20</sup> Fig. 6 shows the photocatalytic cycle for the partial oxidation of alcohols with this catalyst.

Primary and secondary benzylic alcohols have been oxidized to the corresponding aldehydes and ketones in high yields when H<sub>3</sub>PW<sub>12</sub>O<sub>40</sub> entrapped into a ZrO<sub>2</sub> matrix is used.<sup>20</sup> The reaction proceeds with a selectivity of *ca.* 90% after 3 h of reaction. Acetonitrile, used as reacting medium, increases the reaction yield up to 93% while other organic solvents give only a yield of 60%.

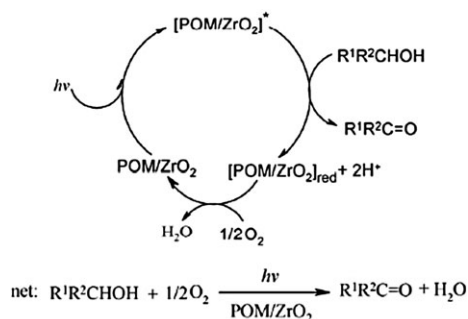


**Fig. 6** The photocatalytic cycle for aerobic oxidation of alcohols by using POM/ZrO<sub>2</sub> as photocatalyst.<sup>20</sup>

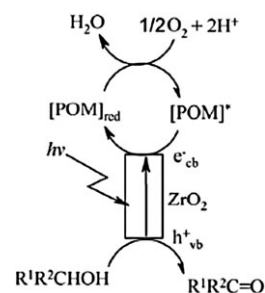


**Fig. 7** Synergistic effect between the POM molecule and the semiconductor in the nanocomposite.<sup>20</sup>

It is worth noting that this reaction is highly selective in partial oxidation of *vic*-diols, obtaining the oxidation of the secondary OH group of benzene ring.<sup>20</sup>

The presence of the POM/ZrO<sub>2</sub> gave rise to an enhanced activity of the POM due to an alternative mechanism where an electron transfer occurred from the conduction band of the zirconia to the UV activated POM affording the reduced POM species (Fig. 7). Such electron transfer can inhibit the electron-hole recombination and the hole on ZrO<sub>2</sub> has sufficient time to oxidize organic substrates. On the other hand POM/semiconductor binary material shows a synergistic effect between the two components.

W<sub>10</sub>O<sub>32</sub><sup>4-</sup> is a polyanion able to induce the photocatalytic oxidation of alcohols in homogeneous regime but also supported on polymeric membranes or mesoporous silica. When the substrate is a diol, a preferential partial oxidation of one of the alcoholic functionalities occurs giving rise to hydroxyaldehydes or hydroxyketones.<sup>21</sup> Analogously to PW<sub>12</sub>O<sub>40</sub><sup>3-</sup>, W<sub>10</sub>O<sub>32</sub><sup>4-</sup> produces, when irradiated, an excited state species which decays rapidly to a reactive transient designed as wO, that reacts with an aliphatic or aromatic alcohols through hydrogen abstraction leading to the reduced HW<sub>10</sub>O<sub>32</sub><sup>4-</sup> species and to an organic radical that reacts with dioxygen giving rise to the carbonylic final product (Fig. 8).

The site selective adsorption of the substrate on the polyanion surface is the basic requirement for a good regioselectivity; this feature can be tuned by controlling the polarity of the environment. The inset of Fig. 9 reports the anchoring of the POM onto the SiO<sub>2</sub> surface by an ionic bond with alkylammonium cations. The photocatalytic oxidation of 1,3-butanediol and 1,4-pentanediol with SiO<sub>2</sub>-bound W<sub>10</sub>O<sub>32</sub><sup>4-</sup> (Fig. 9) gives rise mainly to 4-hydroxy-2-butanone (1b) and 4-hydropentanal (2a) in equilibrium with its emiacetalic

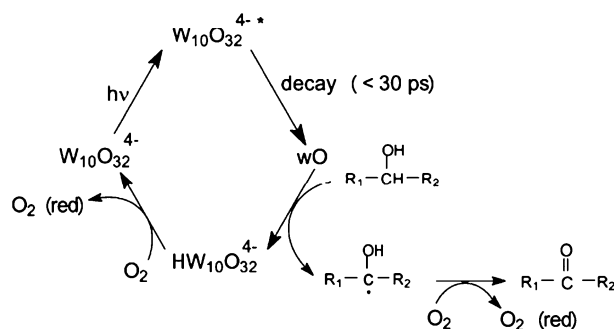


**Fig. 8** Photocatalytic behaviour of W<sub>10</sub>O<sub>32</sub><sup>4-</sup>.<sup>21</sup>

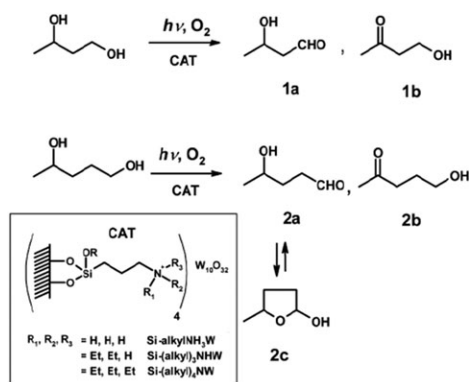


**Fig. 9** Products obtained in the partial oxidation of diols by using  $\text{W}_{10}\text{O}_{32}^{4-}/\text{SiO}_2$  in  $\text{CH}_2\text{Cl}_2$  medium.<sup>21a</sup>

form (2c), respectively, with selectivities of 90 and 80%. 3-Hydroxybutanal (1a) and 5-hydroxy-2-pentanone (2b) were obtained as minor products. It is worth noting that no formation of ketoacids or  $\text{CO}_2$  was observed.<sup>21a</sup>

The photocatalytic oxidation of 1,4-pentanediol has been also investigated in UV-illuminated acetonitrile suspensions of  $\text{ZrTiO}_4$  powder under oxygenated conditions.<sup>21b</sup> A virtually total regiochemical preference for oxidation of the primary hydroxyl group in 1,4-pentane diol was found and 4-hydroxy-pentanoic acid and its  $\gamma$ -lactone derivative were the sole products.

## 1.2 Partial oxidation of alkenes

Epoxidation of olefins is one of the most important functional group transformations in organic synthesis. Photocatalytic epoxidation processes have been studied extensively, especially by using  $\text{TiO}_2$ , however the process exhibits a low epoxide selectivity.

Partial oxidation of cyclopentene was carried out by using a series of commercial and sol-gel home prepared  $\text{TiO}_2$  samples.<sup>22</sup> The reaction pathway is reported in Fig. 10.

Cyclopentenylhydroperoxide (A) is found to be the initial intermediate for all the reaction pathways: 6-oxabicyclo[3.1.0]hexane (C) and cyclopent-2-en-1-one (B) are the main products along with penta-1,5-dial (glutaraldehyde) (D), that represents only ca. 9% of the total amount of products. The total oxidation of the alkene to  $\text{CO}_2$  also occurs in a 17–27 wt%. Similar results were obtained by using cyclohexane.<sup>23</sup> Cyclohexenylhydroperoxide is the common initial intermediate which gives rise mainly to two parallel reaction pathways, generating the epoxide and the aldehyde, similarly to the products formed by cyclopentene.

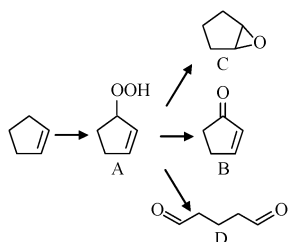


**Fig. 10** Reaction pathway of the partial oxidation of cyclopentene.<sup>22</sup>

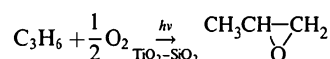


**Fig. 11** Photocatalytic oxidation of propene over  $\text{TiO}_2\text{-SiO}_2$  catalysts.<sup>27</sup>

The use of commercial or home prepared  $\text{TiO}_2$  samples has a strong influence on the yield and selectivity of this process. Kluson *et al.*<sup>22</sup> report that, when commercial powders were used, the main product obtained was the ketone (selectivity in the range 35 to 49%), on the contrary with the sol-gel prepared powders the epoxide was mainly obtained (selectivity 26 to 49%). The commercial samples showed, in general, lower photoactivity than the home prepared ones. A plausible explanation of these features invokes two mechanisms of surface reaction: (i) the first one involves the formation of hydroxyl radicals through the contact of positively charged electron vacancies with adsorbed surface water and it is responsible for the mineralization reaction; (ii) the second mechanism involves a series of transformations started by reaction of  $\text{O}_2$  with photogenerated electrons. This reductive mechanism, producing a number of active species such as surface hydroperoxide or singlet oxygen, would be responsible for the epoxidation reaction.

Epoxidation of propene is a reaction of paramount importance in the chemical industry. It has been reported that metal oxide species, when they are highly dispersed on silica, alumina, mesoporous silica or zeolites, exhibit photocatalytic activity for partial oxidation reactions.<sup>24</sup>  $\text{TiO}_2\text{-SiO}_2$  with low  $\text{TiO}_2$  content is active in yielding propylene oxide from propene by molecular oxygen (Fig. 11) at room temperature with a selectivity of 60%.<sup>25</sup> When the highly dispersed active sites are quantum sized isolated metal oxide species, as isolated tetrahedral  $\text{TiO}_4$  on silica, these species could promote selective oxidations.<sup>26</sup> The excited state is localized at the isolated quantum sized metal oxides, well characterized by their phosphorescence emission.<sup>27</sup> The *quantum photocatalysts* can induce epoxidation of propene by molecular oxygen but also direct methane coupling or photomethathesis of olefines.

Many species dispersed on silica are able to produce propylene oxide from propene.<sup>28</sup> The highly dispersed (isolated) tetrahedral species of  $\text{TiO}_2$ <sup>25</sup> or  $\text{ZnO}$ <sup>28</sup> quantum sized on  $\text{SiO}_2$  show a 60% selectivity with a 4.4% conversion and a 33.7% selectivity with a 8.6% conversion, respectively. In both cases the active phases are atomically dispersed tetrahedral metal oxide species. Visible light photocatalytic production of propylene oxide has been also reported by using  $\text{Cr}_2\text{O}_3\text{-SiO}_2$  system<sup>29</sup> where highly dispersed Cr species acted as active sites giving rise to a selectivity of 32% at 7% conversion.

## 1.3 Cyclohexane partial oxidation and dehydrogenation

Partial oxidation of cyclohexane is an important reaction particularly in its conversion to cyclohexanone and then to caprolactam, monomer for the nylon-6 production. The other possibility is cyclohexanol dehydration to cyclohexanone, but this is a costly and consuming energy process so the first way is preferred.

Du *et al.*<sup>30</sup> have studied the cyclohexane partial oxidation by photolysis and photocatalysis. The photolysis reaction occurs

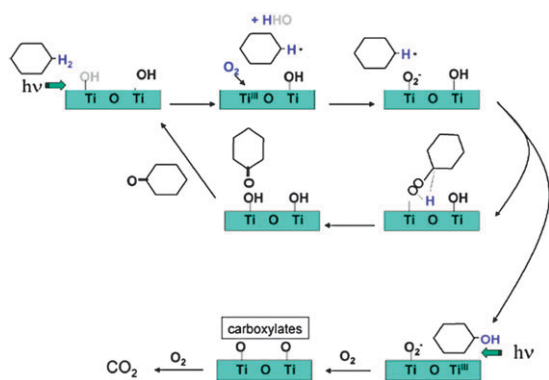


**Fig. 12** Reaction mechanism proposed<sup>30</sup> for the photocatalytic production of cyclohexanone over TiO<sub>2</sub> catalysts.

only by irradiating the homogeneous system with UVC light ( $\lambda < 280$  nm) and cyclohexanol is mainly obtained with small amounts of cyclohexanone and 1,1'-oxybis(cyclohexane), which is produced by the etherification reaction of two cyclohexanol molecules. The addition of TiO<sub>2</sub> Degussa P25 under the same UV irradiation decreases the amounts of products of *ca.* one order of magnitude and moreover it changes the product distribution, cyclohexanone being the main product and cyclohexanol the minor one. When the TiO<sub>2</sub> suspension is irradiated with near-UV light ( $\lambda > 280$  nm), an almost complete selectivity to cyclohexanone was obtained (>95%).

The mechanism invoked by Du *et al.*<sup>30</sup> for explaining the parallel formation of cyclohexanol and cyclohexanone is reported in Fig. 12. In this mechanism the hydroxyl groups on the photocatalyst surface play an important role as they are directly involved in the photooxidation of cyclohexane to cyclohexanol.

The conversion and selectivity of cyclohexane oxidation are dependent on the solvent medium and the oxygen flow. Vinu *et al.*<sup>31</sup> have conducted the reaction in a chloroform medium obtaining a selectivity to cyclohexanone of 63% with a 9% conversion by using a combustion synthesized Ti<sub>0.99</sub>Ag<sub>0.01</sub>O<sub>2- $\delta$</sub> .

Maldotti *et al.*<sup>32</sup> have used a mesoporous TiO<sub>2</sub> material (MCM type). This innovative kind of TiO<sub>2</sub> samples was prepared by preformed nanoparticles that, after adequate stabilization by ligands and templation with surfactants,<sup>33</sup> produce mesoporous TiO<sub>2</sub> more robust than those prepared by titanium isopropoxide. The products obtained in pure cyclohexane are cyclohexanol and cyclohexanone, both the alcohol and ketone concentrations increase by increasing the TiO<sub>2</sub> amount in the framework that contains also SiO<sub>2</sub>. The oxidation of cyclohexane in the presence of TiO<sub>2</sub> Degussa P25 is faster but less selective than by using the mesoporous material.

Recently Ciambelli *et al.* have studied the photocatalytic reaction of cyclohexane in gas–solid regime in the presence of O<sub>2</sub>, obtaining cyclohexene and benzene by oxidative dehydrogenation.<sup>34,35</sup> These products are very different from those obtained in aerobic liquid–solid regime.

## 2. Reduction

While the total or partial oxidation of organic compounds is largely studied because the most common semiconductor

photocatalysts have valence band edges that are more positive than oxidation potentials of most organic functional groups, photocatalytic reductions are less frequently found because the reducing power of a conduction band electron is significantly lower than the oxidizing power of a valence band.<sup>36</sup>

Photocatalytic reduction of organic acceptors can be carried out in the presence of a large excess of an electron donor, such as methanol, and in the absence of O<sub>2</sub>.<sup>37–39</sup> The purpose of the electron donor is to scavenge holes, thereby reducing the degree of recombination within the particle. As oxygen is a competitive electron scavenger, de-oxygenation of the system is necessary to improve reduction efficiency. From the point of view of eco-friendly production of chemicals, attention must be paid to the choice of solvent and sacrificial reagents for photocatalytic reduction of organic compounds. Methanol has been used as both a solvent and a sacrificial reagent; however, since formaldehyde is formed as the oxidized species of methanol, a sacrificial reagent converting to a non-toxic compound is preferable.

### 2.1 CO<sub>2</sub> reduction

Photocatalytic CO<sub>2</sub> reduction has been receiving much attention because of the environmental problems caused by the continuously increasing CO<sub>2</sub> concentration in the atmosphere. Therefore the efficient photoreduction of CO<sub>2</sub> is one of the most challenging tasks of environmental catalysis. It must be considered also that CO<sub>2</sub> is an inexpensive, non-flammable and non-toxic carbon source so it is highly desirable to be able to convert it into useful carbon products.<sup>40</sup> After the first report on photocatalytic reduction of CO<sub>2</sub> in water,<sup>41</sup> the light induced reduction of CO<sub>2</sub> has been performed under UV irradiation using TiO<sub>2</sub><sup>42,43</sup> in the presence of a hole scavenger or with silica containing highly dispersed Ti-oxide species. A number of zeolites and mesoporous molecular sieves have been also employed and TiO<sub>2</sub>/SiO<sub>2</sub> mixed mesoporous thin films showed higher reduction yields and quantum yields than the powdered catalysts.

Besides the usual TiO<sub>2</sub> material, colloidal particles of ZnS have been used<sup>44</sup> to reduce aqueous CO<sub>2</sub> under ultraviolet irradiation in the absence or presence of a Na<sub>2</sub>S solution (containing both aqueous H<sub>2</sub>S and HS<sup>–</sup>) which served as a valence-band hole scavenger. Inorganic carbon was introduced into the reaction mixture or by bubbling CO<sub>2</sub> or in some cases by adding NaHCO<sub>3</sub>. Formate ion was the main photoproduct but also acetate and propionate ions were formed, a finding which demonstrated the formation of carbon–carbon coupling products. The CO<sub>2</sub> photoreduction rate increased by increasing the pH of the solution in the 5–9 range. The initial rate of formate production was proportional to the concentration of aqueous inorganic carbon suggesting an absence of surface saturation. In the absence of hole scavenger but in the presence of the ZnS colloid, the formate production rate drastically decreased.

It still remains a challenge, however, to find how CO<sub>2</sub> photoreduction can be efficiently carried out using the visible-light. TiO<sub>2</sub> semiconductor, in its anatase form, has a relatively large band gap of 3.2 eV, corresponding to wavelengths shorter than 388 nm and thus it makes use of only



3–4% of the solar energy that reaches the earth, demanding a UV light source to be used as a photocatalyst. Consequently the width of absorption wavelengths of  $\text{TiO}_2$  has been obtained by preparing nano-sized  $\text{TiO}_2$  particles,  $\text{TiO}_2$  thin films, highly dispersed titanium oxide species within the zeolite cavities, titanium oxide-based binary catalysts, by loading metal ions on the surface of  $\text{TiO}_2$  particles or with other methods.<sup>45–49</sup>

Phthalocyanines (Pc-s) are a class of organic compounds which have received considerable attention from scientists because of their excellent properties of semi-conductivity, photoconductivity, chemical stability and optical absorption in the UV and visible region.<sup>50,51</sup> Most of the studies conducted so far on Pc-s are either in film, vapor or in any solvent medium, whereas only a limited amount of work has been reported in solid matrices.<sup>52,53</sup> Anchoring of the dye complex to the nanocrystalline semiconductors enables ultrafast injection of electrons from the excited state into the conduction band of semiconductors and the efficiency of photon-to-current conversion improves.

The photoreduction of  $\text{CO}_2$  using sol–gel derived  $\text{TiO}_2$ -supported zinc or cobalt-phthalocyanine has been reported;<sup>54</sup> these catalysts can reduce  $\text{CO}_2$  under visible light but the yield of product is low.

In order to increase the yield, transition-metal complexes are used as catalysts since they can absorb a significant part of the solar spectrum and have long-lived excited states. Supported  $\text{ZnPc-TiO}_2$  catalysts have been tested<sup>55</sup> for the photo-reduction of  $\text{CO}_2$  under visible light illumination. The catalysts were prepared by an improved sol–gel technique illustrated in Fig. 13.

The BH-1  $\text{TiO}_2$  powder is a commercial one and was tested for comparison aims.  $\text{ZnPc}$ -loaded  $\text{TiO}_2$  ( $\text{ZnPc/TiO}_2$  and  $\text{ZnPc/BH-1}$ ) have been impregnated by adding  $\text{ZnPc}$  during the sol–gel process. An *in situ* chemical synthesis technique was successfully used to synthesize  $\text{ZnPc}$  in a sol–gel matrix (*in situ*  $\text{ZnPc/TiO}_2$ ).

The photo-catalytic reduction was carried out in a Pyrex glass cell containing the catalyst powder suspended in  $\text{NaOH}$  aqueous solution in which  $\text{CO}_2$  was continuously bubbled. Illuminations were performed with a 500-W tungsten-halogen

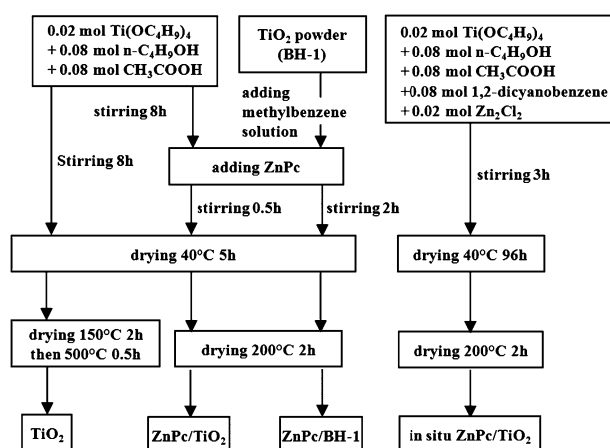


Fig. 13 Procedure for catalyst preparation.<sup>55</sup>

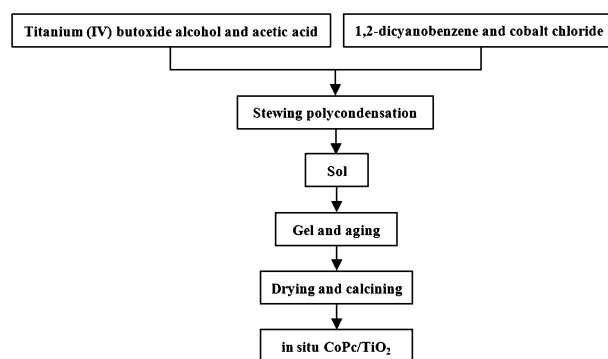


Fig. 14 Procedure for catalyst preparation.<sup>56</sup>

lamp. The optimal  $\text{CO}_2$  conversion in this system is 0.37%;  $\text{HCOOH}$ ,  $\text{CO}$  and  $\text{CH}_4$  were produced, the formation of formic acid being more effective on supported  $\text{ZnPc/TiO}_2$  catalyst than on  $\text{TiO}_2$  catalyst.

The Authors report that the activity of the catalysts followed the order: *in situ*  $\text{ZnPc/TiO}_2$  > 1.0 wt%  $\text{ZnPc/TiO}_2$  >  $\text{ZnPc/BH-1}$  > 3.0 wt%  $\text{ZnPc/TiO}_2$  > 5.0 wt%  $\text{ZnPc/TiO}_2$  >  $\text{TiO}_2$ . The results indicate that  $\text{ZnPc}$  is an effective photo-sensitizer, able to produce electrons and to effectively absorb visible light. The electrons excited are transferred to  $\text{TiO}_2$  and reduce  $\text{CO}_2$ , at the same time the recombination of electron-hole pairs is reduced.

Cobalt-phthalocyanine (CoPc) has been also supported on  $\text{TiO}_2$ <sup>56</sup> by an *in situ* method and the  $\text{CO}_2$  photoreduction has been studied in  $\text{NaOH}$  aqueous solution by achieving the formation of  $\text{HCOOH}$ ,  $\text{HCHO}$  and  $\text{CH}_3\text{OH}$  under visible light. *In situ*  $\text{CoPc/TiO}_2$  is prepared with the advanced sol–gel procedure illustrated in Fig. 14. For comparison, the  $\text{CoPc/TiO}_2$  catalysts are prepared by equilibrium adsorption of CoPc on  $\text{TiO}_2$  from a solution of dimethylformamide.

Formic acid, methanol and formaldehyde are produced on  $\text{CoPc/TiO}_2$  catalyst; their yields, reported in Table 3, demonstrate that an optimal *in situ* synthesized  $\text{CoPc/TiO}_2$  is a highly efficient photocatalyst for  $\text{CO}_2$  reduction.

The location of CoPc on  $\text{TiO}_2$  plays an important role in the photoreduction of  $\text{CO}_2$ . Isolated CoPc is regarded as the primary active site for photoreduction. The distribution of CoPc on  $\text{TiO}_2$  particles is critical to maximize the yield of reduction products. CoPc under visible light irradiation produces electron-hole pairs and  $\text{TiO}_2$  serves as an electron trapper then hindering the electron-hole recombination. At the same time,  $\text{CO}_2$  can accept an electron on  $\text{TiO}_2$  surface and be reduced to  $\text{HCOOH}$ ,  $\text{HCHO}$  and  $\text{CH}_3\text{OH}$ .

Another way for widening the  $\text{TiO}_2$  absorption towards the visible region is the use of dye sensitizers. A recent study<sup>57</sup> provides evidence that dye sensitized, Pt promoted  $\text{TiO}_2$  films

Table 3 Yield of various catalysts<sup>56</sup>

	Production yield [ $\mu\text{mol (g}_{\text{cat}})^{-1}$ ]			
	$\text{HCOOH}$	$\text{CH}_3\text{OH}$	$\text{HCHO}$	TOC
$\text{TiO}_2$	221.0	—	—	221.0
1.0 wt% $\text{CoPc/TiO}_2$	450.6	12.1	38.5	501.2
0.7 wt% <i>in situ</i> $\text{CoPc/TiO}_2$	1487.6	93.0	134.3	1714.9

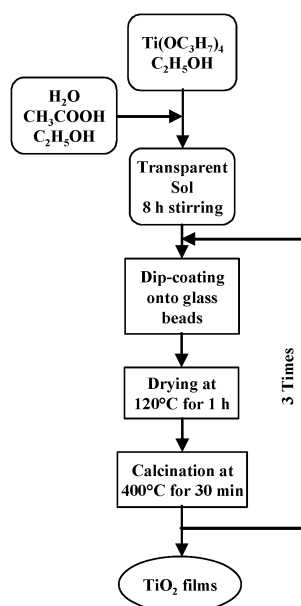


Fig. 15 Flow chart for the TiO<sub>2</sub> film coating procedure.<sup>57</sup>

are capable of CO<sub>2</sub> reduction under visible light excitation and in the presence of water vapour. In order to induce dye sensitization, perylene diimide derivatives and a commercial reference compound were used.

TiO<sub>2</sub> films were coated on regular borosilicate glass beads *via* a sol–gel procedure. A flow diagram is given in Fig. 15 summarizing the steps and the ingredients used in the film coating procedure.

Two types of Pt promoted films, Pt(on) and Pt(in) films, were prepared to see the effect of Pt addition procedure on the photocatalytic performance of the films. Pt(on) catalysts were prepared using aqueous solutions of Pt containing salt and Pt was added on a TiO<sub>2</sub> support *via* wet impregnation technique. On the other hand for Pt(in) catalysts, Pt salt was added to the TiO<sub>2</sub> coating sol, so that Pt was added to TiO<sub>2</sub> framework.

Three different light harvesting molecules (LHM) were used: Tris(2,2′-bipyridyl) ruthenium(II) chloride (RuBpy), 1,7-dibromo-*N,N'*-(carboxymethyl)-3,4:9,10-perylene-diimide (BrGly) and 1,7-dibromo-*N,N'*-(1S,2-dicarboxyethyl)-3,4:9,10-perylene-diimide (BrAsp). The reaction tests are carried out in a batch photoreactor irradiated by a daylight lamp.

The aim of synthesizing LHM promoted TiO<sub>2</sub> films was to combine the visible light excitation potential of the organic dyes with the catalytic performance of TiO<sub>2</sub>. The excited state electrons on the dye molecule can be injected to the TiO<sub>2</sub> structure thus determining photocatalytic activity in the visible region. The reaction tests of RuBpy–TiO<sub>2</sub>, BrGly–TiO<sub>2</sub> and BrAsp–TiO<sub>2</sub> thick film catalysts showed that the excitation–injection mechanism is working successfully. Methane production is observed, the activities being in the order of BrAsp–TiO<sub>2</sub> > RuBpy–TiO<sub>2</sub> > BrGly–TiO<sub>2</sub>.

In the presence of Pt, all three sensitizers showed photocatalytic activity in the visible region. Addition of Pt *via* aqueous solution resulted in the catalysts with highest methane yields while addition of Pt *via* Pt containing sol resulted in either no significant change or even decrease in photocatalytic

activity. The presence of Pt in the bulk of TiO<sub>2</sub> may modify the band gap and indeed improve the TiO<sub>2</sub> activity.<sup>57</sup> The electron transfer efficiencies from the dye sensitizer to the TiO<sub>2</sub> can increase in the presence of Pt; furthermore, the dye compounds can bind better to the structure in the presence of Pt and it is highly possible that more dye sensitizers could have been incorporated on the films in the presence of Pt.

Inspired by the photosynthesis of plants, Ozcan *et al.*<sup>58</sup> studied the effect of an organic dye adsorbed on photocatalyst on the CO<sub>2</sub> photoreduction with H<sub>2</sub>O to fuels under artificial light. However, the employment of organic dye limited the efficiency of the system.

On these grounds the CO<sub>2</sub> reduction has been investigated<sup>59</sup> over Ruthenium dye-sensitized TiO<sub>2</sub>-based catalysts under artificial light and concentrated natural sunlight. The photocatalytic runs were carried out in a continuous circular Pyrex glass reactor containing catalyst-coated optical fibres on whose surface the photocatalytic reaction is conducted. Optical fibres allow to overcome the several drawbacks presented by the liquid-phase photoreactor, such as low light utilization efficiencies due to absorption and scattering of the light by the reaction medium and in some cases the rates are low due to limitations by mass transport resistances. Packed-bed photoreactor irradiated either from side or center always projects shadow on the other side of catalyst particle and thus an aliquot of photocatalyst surface is not active. In order to solve these problems, Marinangeli and Ollis<sup>60,61</sup> proposed to use optical fibers as a means of light transmission and distribution to solid-supported photocatalysts. An optical fiber provides a very high exposure surface and allows to deliver photons uniformly in a large volume.

P25 titanium dioxide was used as a TiO<sub>2</sub> source. Cu(NO<sub>3</sub>)<sub>2</sub>·3H<sub>2</sub>O and Fe(NO<sub>3</sub>)<sub>3</sub>·9H<sub>2</sub>O were employed as precursors of metal dopants and Ru<sup>II</sup>(2,20-bipyridyl-4,40-dicarboxylate)2-(NCS)<sub>2</sub> (hereafter indicated as N3) was used as dye sensitizer. The optical fibers were coated with TiO<sub>2</sub> slurry containing the corresponding metal salts by dip coating method. For comparison aims the catalysts were also supported on glass plates. The photocatalytic reaction was carried out in a continuous circular Pyrex glass reactor. The products of CO<sub>2</sub> reduction were methane and ethylene; their rates of production under artificial light are reported in Table 4.

N3 dye adsorbed on TiO<sub>2</sub> catalyst was found to be stable under UV irradiation and therefore the CO<sub>2</sub> photoreduction

Table 4 Production rate of methane and ethylene over TiO<sub>2</sub>-based catalysts under artificial light<sup>59</sup>

	Production rate <sup>a</sup> [μmol (g <sub>cat</sub> ) <sup>-1</sup> h <sup>-1</sup> ]	
	Ethylene	Methane
Cu(0.5 wt%)–Fe(0.5 wt%)/TiO <sub>2</sub> /glass plate	0.049	0.060
Cu(0.5 wt%)–Fe(0.5 wt%)/TiO <sub>2</sub> /optical fiber	0.575	0.914
N3-dye–Cu(0.5 wt%)–Fe(0.5 wt%)/TiO <sub>2</sub> /glass plate	0.033	0.148
N3-dye–Cu(0.5 wt%)–Fe(0.5 wt%)/TiO <sub>2</sub> /optical fiber	0.562	0.847

<sup>a</sup> Production rates were determined on the basis of the average value after 4 h of irradiation. The artificial light was in the wavelength range of 320–500 nm with intensity of 225 mW cm<sup>-2</sup>.

proceeds without any loss of activity during irradiation time. This finding indicates that the charge transfer from N3 dye to  $\text{TiO}_2$  is very efficient and N3 results to properly work as a sensitizer.

It is found that production rates of methane and ethylene with catalysts supported on optical fibers are higher than those with glass plates while those rates are similar over both Cu–Fe/ $\text{TiO}_2$  and N3-dye–Cu–Fe/ $\text{TiO}_2$  catalysts thus showing that N3 dye is not effective for the improvement of methane and ethylene production.

For the experiments using concentrated natural sunlight as the irradiation source, only the catalysts supported on optical fibers were tested. Although both methane and ethylene were produced under artificial light, under concentrated natural sunlight only methane production was observed. The methane production rates with Cu(0.5 wt%)-Fe(0.5 wt%)/ $\text{TiO}_2$  and with N3-dye–Cu(0.5 wt%)-Fe(0.5 wt%)/ $\text{TiO}_2$  were 0.281 and 0.617  $\mu\text{mol (g}_{\text{cat}})^{-1} \text{h}^{-1}$ , respectively. N3 dye is observed to increase the photoactivity of Cu–Fe/ $\text{TiO}_2$  catalyst up to over 100% under concentrated natural sunlight. The superior photoproduction of dye adsorbed catalyst could be ascribed to the strong absorption of N3 dye in the visible range.

Catalysts different from the  $\text{TiO}_2$ -based ones have been also tested. Pan and Chen<sup>62</sup> tested  $\text{InTaO}_4$  and  $\text{NiO/InTaO}_4$  as catalysts for  $\text{CO}_2$  photoreduction in liquid water under visible light irradiation. The polycrystalline  $\text{InTaO}_4$  was synthesized by solid state reaction at high temperature with  $\text{In}_2\text{O}_3$  and  $\text{Ta}_2\text{O}_5$  as the starting materials. In order to improve the photogenerated electrons trapping and so to obtain high photocatalytic activity, a metal oxide acceptor,  $\text{NiO}$ , was loaded at different percentages on the surface of the photocatalyst by incipient-wetness impregnation. It is believed that the co-catalyst works as an electron trap, and the surface becomes a Schottky barrier able to suppress the electron-hole recombination.

The  $\text{InTaO}_4$  compound shows absorption in visible light region up to 465 nm, thus showing that  $\text{InTaO}_4$  has the ability to respond to the visible light irradiation. The band gap of  $\text{InTaO}_4$  is 2.6 eV and it does not change for the addition of  $\text{NiO}$  cocatalyst; on the contrary the absorbance of  $\text{InTaO}_4$  increases with the addition of cocatalyst. The band structure of  $\text{InTaO}_4$  (Fig. 16) reveals that  $\text{InTaO}_4$  can reduce  $\text{CO}_2$  under the visible light irradiation.

Photocatalytic reactions were carried out in a semi-continuous reactor. The catalyst powder was dispersed in  $\text{KHCO}_3$  aqueous solution employed as  $\text{CO}_2$  absorbent and the ultra pure  $\text{CO}_2$  was continuously bubbled to remove oxygen and to saturate the solution.

Methanol was the only product detected from  $\text{CO}_2$  photoreduction. The highest methanol yield was obtained with 1.0 wt%  $\text{NiO-InTaO}_4$ . The performance of the system was evaluated by determining the quantum and energy efficiencies. By considering that 6 moles of electrons are required to produce 1 mole of methanol from  $\text{CO}_2$ , the quantum efficiency is defined as:

$$\text{Quantum efficiency} = \frac{6 * \text{moles of produced methanol}}{\text{moles of absorbed photons}} \quad (1)$$

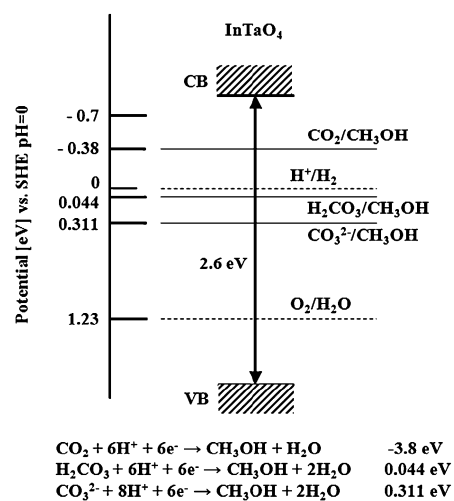


Fig. 16 Band structure of  $\text{InTaO}_4$ .

The energy efficiency, which evaluates the transformation of the photon energy into chemical energy, is defined as:

$$\text{Energy efficiency} = \frac{\text{heat of combustion of produced methanol}}{\text{energy of visible radiation absorbed}} \quad (2)$$

The quantum efficiency and energy efficiency were 2.45% and 1.158%, respectively.

Liu *et al.*<sup>63</sup> studied the selective ethanol formation from  $\text{CO}_2$  photocatalytic reduction in water with  $\text{BiVO}_4$  photocatalyst. Monoclinic bismuth vanadate is a photocatalyst for  $\text{O}_2$  production from water under visible light irradiation. This reaction suggests that the photogenerated holes of  $\text{BiVO}_4$  are consumed by water to produce  $\text{O}_2$ . The byproducts of this reaction are photogenerated electrons and protons. Since the photogenerated electrons are not able to capture the protons in water to form  $\text{H}_2$ , the possibility of using the photo-generated electrons and protons for converting  $\text{CO}_2$  to organic compounds has been tested. Liu *et al.*<sup>63</sup> demonstrated the feasibility of this process in aqueous dispersions of  $\text{BiVO}_4$  (tetragonal or monoclinic) powder and they found that  $\text{CO}_2$  photoreduction leads selectively to ethanol.  $\text{BiVO}_4$  powder, prepared by microwave assisted hydrothermal method,<sup>64,65</sup> was dispersed in water and  $\text{CO}_2$  was continuously bubbled through the solution. 300W Xe arc lamp with and without UV cut off filter were used for the irradiation.

Monoclinic  $\text{BiVO}_4$  exhibits a much higher photocatalytic activity than tetragonal  $\text{BiVO}_4$ . The reactivity data, reported in Table 5, indicate that, when the irradiation light is extended into the UV region, the rate of the ethanol production strongly increases for monoclinic  $\text{BiVO}_4$ . Moreover the intensity of the light irradiation plays an important role in the ethanol formation because both methanol and ethanol are formed with comparable rates when a 36 W fluorescent lamp is used.

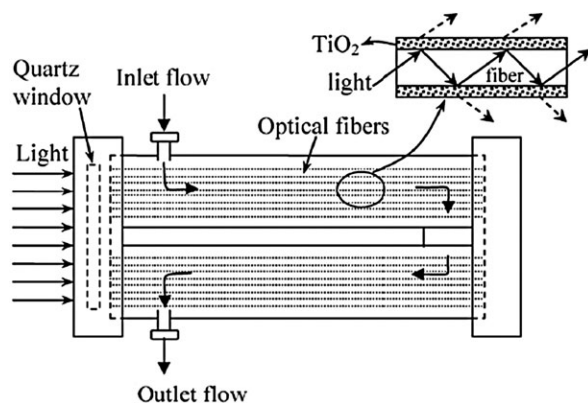
The  $\text{CO}_2$  photoreduction to hydrocarbons in gaseous phase has been carried out by using optical fibres coated with Cu–Fe/ $\text{TiO}_2$  catalyst.<sup>66</sup>

P25 was used as a  $\text{TiO}_2$  source.  $\text{Cu}(\text{NO}_3)_2 \cdot 3\text{H}_2\text{O}$  and  $\text{Fe}(\text{NO}_3)_3 \cdot 9\text{H}_2\text{O}$  were employed as precursors of metal dopants on  $\text{TiO}_2$  support. Photocatalytic runs were carried

**Table 5** Rates of ethanol and methanol production under three different light-irradiation conditions<sup>65</sup>

		300 W Xe arc lamp with UV cutoff filter	300 W Xe arc lamp without UV cutoff filter	36 W fluorescent lamp
BiVO <sub>4</sub>	Production rate <sup>a</sup> /μmol h <sup>-1</sup>			
Monoclinic	Ethanol	21.6	406.6	2.3
	Methanol	0	0	1.8
Tetragonal	Ethanol	1.1	4.9	0.6
	Methanol	0	0	0.6

<sup>a</sup> The rate was determined on the basis of the average production rate after 80 min of irradiation.

**Fig. 17** Continuous circular Pyrex glass reactor. (Reproduced with permission from ref. 66).

out in a continuous circular Pyrex glass reactor shown in Fig. 17. Catalyst coated optical fibres were irradiated by UVA (320–500 nm) and UVC (250–450 nm) light obtained by using appropriate filters on the Hg high pressure lamp. For comparison, the photocatalytic conversion of CO<sub>2</sub> into hydrocarbons was also studied on glass plates coated with the same catalysts.

Cu–Fe/TiO<sub>2</sub> catalysts were able to photoreduce CO<sub>2</sub> with H<sub>2</sub>O vapour to ethylene and methane; traces of ethane and methanol were also found. Table 6 presents the production rate of ethylene over different photocatalysts and supports under UVC (250–450 nm).

Pure TiO<sub>2</sub> shows negligible photocatalytic activity towards ethylene production while, when either Cu or Fe is loaded, the

**Table 6** Production rate of ethylene over different photocatalysts and carriers under UVC<sup>66</sup>

	Ethylene production rate <sup>a</sup> [μmol (g <sub>cat</sub> ) <sup>-1</sup> h <sup>-1</sup> ]	
	Over glass plate	Over optical fiber
TiO <sub>2</sub> -P25	0.00	0.00
Cu(1wt%)/TiO <sub>2</sub>	0.01	0.24
Fe(1wt%)/TiO <sub>2</sub>	0.02	0.08
Cu(1 wt%)-Fe(1 wt%)/TiO <sub>2</sub>	0.04	0.35
Cu(0.5 wt%)-Fe(0.5 wt%)/TiO <sub>2</sub>	0.05	0.58
Cu(0.25 wt%)-Fe(0.25 wt%)/TiO <sub>2</sub>	0.03	0.53

<sup>a</sup> Production rates were determined on the basis of the average value after 4 h of irradiation. The artificial light was in the wavelength range of 250–450 nm with intensity of 225 mW cm<sup>-2</sup>.

**Table 7** Ethylene production rate over different catalysts under UVA<sup>66</sup>

	Production rate <sup>a</sup> over glass plate [μmol(g <sub>cat</sub> ) <sup>-1</sup> h <sup>-1</sup> ]	
	Ethylene	Methane
TiO <sub>2</sub> -P25	0.00	Trace
Cu(1wt%)/TiO <sub>2</sub>	0.01	0.09
Fe(1wt%)/TiO <sub>2</sub>	0.02	0.06
Cu(1 wt%)-Fe(1 wt%)/TiO <sub>2</sub>	0.04	0.06
Cu(0.5 wt%)-Fe(0.5 wt%)/TiO <sub>2</sub>	0.05	0.06
Cu(0.25 wt%)-Fe(0.25 wt%)/TiO <sub>2</sub>	0.01	0.19

<sup>a</sup> Production rates were determined on the basis of the average value after 4 h of irradiation. The artificial light was in the wavelength range of 320–500 nm with intensity of 225 mW cm<sup>-2</sup>.

derived catalysts are able to reduce CO<sub>2</sub> to ethylene. Moreover, as Cu and Fe are employed as co-dopants on the TiO<sub>2</sub> support, a synergistic effect appears; the optimum amount of Cu and Fe loading on TiO<sub>2</sub> are 0.5% wt for each. However, the production rate of ethylene on optical fibres is one order of magnitude higher than that on glass plate. This result is ascribed to the efficient charge transfer mechanism between TiO<sub>2</sub> as a support and Cu as well as Fe as co-dopants.

When the catalysts were irradiated by UVA light, the CO<sub>2</sub> photoreduction products were ethylene and methane; the corresponding production rates are shown in Table 7.

From the results reported in Tables 6 and 7, the light source does not substantially affect the production rate of ethylene over the catalyst coated on glass plate.

## 2.2 Nitro-compounds reductions

Heterogeneous photocatalysis has proven to be effective also for reduction reactions concerning nitrogen compounds, from nitrate ion to nitro-compounds. In the first case the benefits have been for the environment while in the case of nitro-compounds a new successful route has been furnished to green chemistry.

The intensive agricultural activities and the massive use of man-made fertilizers have increased the nitrate concentration in water supply sources. High concentration of nitrate in drinking water is fatal to infants in whose bodies nitrate is reduced to nitrite, which combines with hemoglobin in the blood to form methaemoglobin, and leads to a condition commonly known as “blue baby syndrome”. Furthermore, nitrate can be converted into nitrosamine, which can cause cancer and hypertension.

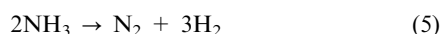
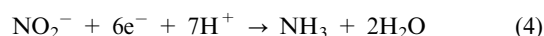
TiO<sub>2</sub>-based catalysts are effective for nitrate reduction. It is known that metal-loaded TiO<sub>2</sub> catalysts with the addition of hole scavengers are essential for the effective reduction of NO<sub>3</sub><sup>-</sup> to NH<sub>3</sub> and traces of NO<sub>2</sub><sup>-</sup> (during the first minutes of irradiation).<sup>67</sup> Many metals, such as Pd, Pt, and Rh, and sacrificial electron donors, such as methanol, ethanol and EDTA, oxalic acid, sodium oxalate, formic acid, sucrose, and humic acid have been commonly used to improve photocatalytic efficiency.

A recent work<sup>68</sup> focuses on the preparation, characterization and application of Bi<sup>3+</sup>-doped TiO<sub>2</sub> photocatalysts for the reductive decomposition of nitrate to form nitrogen in water in



the presence of formic acid as hole scavenger. The  $\text{Bi}^{3+}$ -doped  $\text{TiO}_2$  samples were prepared by a sol-gel method; the photo-reduction runs were carried out in a batch photoreactor of borosilicate glass irradiated by a medium-pressure mercury lamp as a near-UV light source.

Compared to pure  $\text{TiO}_2$ , the  $\text{Bi}^{3+}$ -doped catalyst exhibited a faster rate of nitrate reduction. The optimal amount of  $\text{Bi}^{3+}$  was 1.5 wt%; a higher bismuth content on  $\text{TiO}_2$  was detrimental to the efficiency of photocatalytic reduction of nitrate. In this study<sup>68</sup> formic acid was chosen as a hole scavenger owing to the fact that its oxidation to carbon dioxide is straightforward and involves minimal intermediate products.<sup>69</sup> Moreover formic acid is capable of forming reducing radicals, which could help in the nitrate reduction reaction. In the presence of formic acid, the reduction of nitrate occurs *via* nitrite and ammonia, and eventually releases nitrogen gas:



This investigation confirms that the use of a hole scavenger such as formic acid is an essential condition to carry out this photocatalytic reduction reaction, since no catalytic activity of either  $\text{TiO}_2$  or  $\text{Bi}^{3+}$ - $\text{TiO}_2$  was observed in the nitrate solution without a hole scavenger. On the other hand, it was found that the further increase of formic acid did not increase the catalytic activity significantly, which may result from competition for adsorption between nitrate and formic anions.

The reductive decomposition of  $\text{NO}_3^-$  to  $\text{N}_2$  in water under UV-irradiation has been carried out in the presence of mesoporous hollandite,<sup>70</sup>  $\text{K}_{1.8}\text{Ga}_{1.8}\text{Sn}_{6.2}\text{O}_{16}$  (KGSO). Hollandites have a characteristic one dimensional tunnel structure with a stoichiometry of  $\text{M}^{\text{IV}}\text{O}_2$  containing the rutile type  $\text{MO}_6$  octahedral linkage<sup>71,72</sup> as illustrated in Fig. 18. The tunnels are usually occupied by alkaline or alkaline earth elements introduced in conjunction with the partial replacement of  $\text{M}^{\text{IV}}$  with di- or trivalent cations.

The aqueous suspension of the catalyst is irradiated by UV light as the absorption edge of KGSO is at the wavelength of 340 nm.  $\text{H}^{15}\text{NO}_3$  and  $\text{CH}_3\text{OH}$  as a reducing agent are the reagents introduced into the photoreactor.  $\text{HNO}_3$  labeled for N is used for the reliable detection of nitrogen gas evolved in the course of the photoreaction.

The hollandite reduces  $\text{NO}_3^-$  to  $\text{N}_2$  *via* nitrite formation; the photocatalytic reduction is accompanied by the partial oxidation of  $\text{CH}_3\text{OH}$  to  $\text{HCOOH}$ , according to:



By increasing the irradiation intensity, the formation of nitrite ions is depressed and that of  $\text{N}_2$  enhanced, while the conversion rates of  $\text{NO}_3^-$  and  $\text{HCOOH}$  are not effectively enhanced. Only formic acid is detected as the carbon component derived from  $\text{CH}_3\text{OH}$  conversion. Therefore the partial oxidation of  $\text{CH}_3\text{OH}$  without  $\text{CO}_2$  evolution can be regarded to proceed in conjunction with the reduction of nitrate ion to  $\text{N}_2$ .

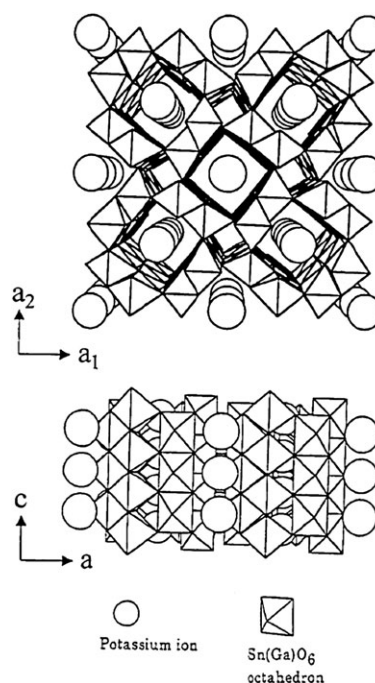
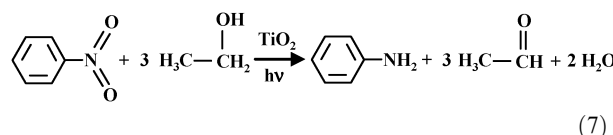


**Fig. 18** Crystal structure of KGSO (Reproduced with permission from ref. 70).

In the case of a photocatalytic reduction of nitrate ion without hole scavenger,  $\text{NO}_3^-$  was slightly converted to  $\text{NO}_2^-$ ,  $\text{N}_2$  molecule being under detectable level.

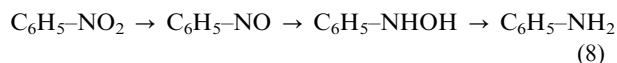
The photocatalytic reduction of nitrobenzene to aniline<sup>73</sup> has been carried out using a large excess of ethanol as a sacrificial electron donor, titanium dioxide and a lamp emitting a broad range of UVA light from 320 to 390 nm with the highest emission at 355 nm.

As shown in eqn (7), the theoretical reaction scheme implies the formation of aniline, acetaldehyde and water as the main products. From a thermodynamic point of view, nitrobenzene reduction is feasible as the reduction potential of nitrobenzene is lower than that of the  $\text{TiO}_2$ . Moreover the photogenerated holes can induce easily the photooxidation of ethanol to acetaldehyde<sup>39</sup> considering the suitable position of oxidation potential of ethanol with respect to that of  $\text{TiO}_2$ . Aniline and acetaldehyde and a small amount of acetic acid were the expected products according to eqn (7), however the intermediates of the photoreduction of nitrobenzene (*i.e.*, nitrosobenzene and N-hydroxylaniline) were also clearly detected.<sup>39,73–75</sup>

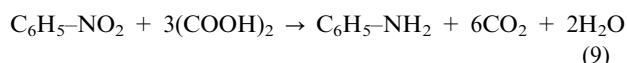


The photocatalytic reduction of nitrobenzene dissolved in an acidic aqueous suspension of P25  $\text{TiO}_2$  was carried out in the presence of oxalic acid as a hole scavenger,<sup>76</sup> the yield of produced aniline was improved in the presence of a small amount of dioxygen. Oxalic acid is a green sacrificial reagent because it is easily oxidized and converts into carbon dioxide which is separated from the solvent under acidic conditions.

After short photoirradiation nitrobenzene was almost completely consumed and aniline was obtained in a high yield, this result indicating that photocatalytic reduction occurred even in the presence of O<sub>2</sub>. Reduction of nitrobenzene to aniline consists of several steps:<sup>37</sup>



and the likely stoichiometry of the reaction in the presence of oxalic acid<sup>76</sup> is:



It is interesting that the yield of aniline in the presence of 2% and 5% O<sub>2</sub> in the gas phase was larger than that in the absence of O<sub>2</sub>; however a further increase in O<sub>2</sub> content in the gas phase decreased the aniline yield: indeed a reoxidation of aniline probably occurred owing to large consumption of oxalic acid in the presence of a high O<sub>2</sub> content.

The production of aromatic amines by photocatalytic reduction emerges as a cost-effective, highly selective, rapid and environmentally friendly process.<sup>77–79</sup>

The N-doped TiO<sub>2</sub> catalyst,<sup>80</sup> which shows good activity under visible light, has been used for the synthesis of amines from nitro compounds. The reduction of aromatic nitro compounds was carried out in the presence of N-TiO<sub>2</sub> and KI in solution of methanol.<sup>81</sup> Photocatalytic runs were carried out in a batch photo-reactor irradiated using high pressure mercury lamp or solar light. The photocatalytic activity of home-prepared (hp) N-doped TiO<sub>2</sub>, undoped hp TiO<sub>2</sub> and TiO<sub>2</sub> Degussa P25 was investigated by the reduction of *o*-nitrophenol as a model reaction; results under UV light, solar light and UV-filtered solar light are shown in Fig. 19. Under UV-filtered solar light only the N-doped TiO<sub>2</sub> showed catalytic activity among the catalysts; under solar and UV irradiation the yield with N-doped TiO<sub>2</sub> was the highest one comparing with hp TiO<sub>2</sub> and P25 TiO<sub>2</sub>.

The reduction of different aromatic nitro compounds has been carried out under UV irradiation because of the long reaction time needed under solar light. The results are listed in Table 8. The data clearly show the efficiency of N-doped TiO<sub>2</sub> in the reduction of several nitro compounds in the presence of KI;

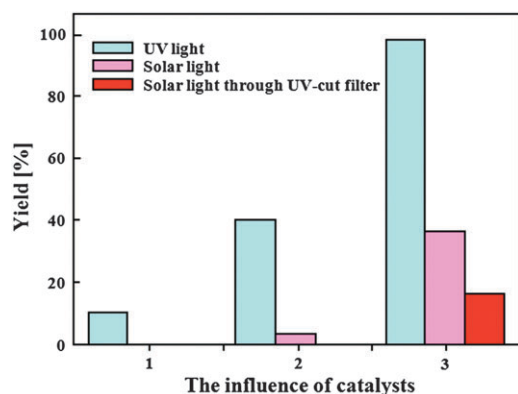


**Fig. 19** The effect of different catalysts: (1) P25; (2) home-prepared TiO<sub>2</sub>; (3) home-prepared N-TiO<sub>2</sub>.<sup>81</sup>

**Table 8** Reduction of functionalized nitroarenes with N-doped TiO<sub>2</sub> and KI<sup>81</sup>

Substrate	Product	Irr. Time/min	Yield(mean ± SD) [%]
		10	99.27 ± 0.21
		12.5	97.77 ± 0.40
		7	99.37 ± 0.35
		10	96.50 ± 0.46
		8.5	97.33 ± 0.47
		7.5	98.07 ± 0.27
		8	95.30 ± 0.75
		11.5	91.95 ± 0.18
		14	98.15 ± 0.71
		7.5	92.06 ± 0.36
		7.5	95.48 ± 0.42
		7.5	97.96 ± 0.27
		7	99.39 ± 0.21
		6	99.47 ± 0.15
		6	91.43 ± 0.29
		19	90.76 ± 0.54

it may be noticed that the reduction of nitroarenes gives corresponding amines in excellent yield (above 90%).

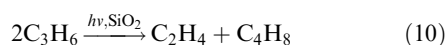
The catalytic system is also efficient in the reduction of aromatic nitro compounds bearing additional substituents in the aromatic ring. With regard to the reactivity of the different nitroarenes tested, it is worth noting that the electronic properties of substituents attached to the aromatic ring do not have any effect on the reduction of nitro groups. Nitro compounds bearing electron-withdrawing groups, which have been reported as more reactive or active when reacted, produce the corresponding amines in better yields and in shorter reaction time with respect to the aromatic nitro compounds substituted with strong-electron releasing groups.

### 3. Other reactions

#### 3.1 Photomethathesis of olefins

The metathesis reaction, consisting of an interchange of carbon atoms between two alkene molecules, is a useful reaction for obtaining alkenes and for their polymerization that is usually performed in the presence of metal catalysts or transition-metal compounds, including various metal carbenes. In this reaction olefins exchange the groups around the double bond, resulting in several outcomes: (i) straight swapping of groups between two acyclic olefins (*cross-metathesis*); (ii) closure of large rings (*ring-closing metathesis*); (iii) formation of dienes from cyclic and acyclic olefins (*ring-opening metathesis*); (iv) polymerization of cyclic olefins (*ring-opening metathesis polymerization*); and (v) polymerization of acyclic dienes (*acyclic diene metathesis polymerization*).<sup>82</sup>

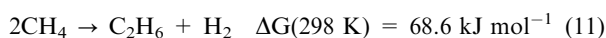
Silica materials, both mesoporous (FSM-16 and MCM-41) and amorphous,<sup>83</sup> show a moderate photocatalytic activity in the propene metathesis reaction when active sites are generated on its surface by dehydroxylation at 673 K.



The reaction produces ethene, *trans*-2-butene, *cis*-2-butene and a small amount of 1-butene. The metathesis reaction seems to be characteristic for the silica surface; in fact, MgO, Al<sub>2</sub>O<sub>3</sub>, SiO<sub>2</sub>-Al<sub>2</sub>O<sub>3</sub> were also tested but, although other reactions occurred to a small extent, the distribution of products was quite different from that for the metathesis reaction.<sup>84</sup>

#### 3.2 Methane coupling

Many studies have been devoted to the appraisal of methane to obtain higher hydrocarbons from this important natural resource. The direct methane coupling producing ethane and hydrogen is a thermodynamically difficult reaction; however it has been carried out photocatalytically by using Al<sub>2</sub>O<sub>3</sub>-SiO<sub>2</sub><sup>85</sup> alone or with the addition of *ca.* 0.5% molar of Ti.<sup>86</sup>



Highly dispersed tetrahedral AlO<sub>4</sub> species were responsible for the important selectivity to ethane, reaching even 90% even if in limited yields (<3%), where Al-O-Si and Al-O-Ti bonds were considered to be the active species. In the case of highly dispersed Zr species on SiO<sub>2</sub> also the phosphorescence emission band of Zn-O-Si was directly related to the photocatalytic

production of ethane from methane. Zeolites<sup>87</sup> also showed a good photocatalytic activity for this reaction.

#### 3.3 N-containing compounds: C-N formation

Azides compounds are commonly used in organic chemistry to introduce an amine group. These atoxic molecules in irradiated homogeneous systems give rise to a mixture of products. The photocatalytic reaction of aromatic azides allows to obtain 2-alkylbenzimidazoles and indole with high yield and under mild conditions.

Selvam *et al.*<sup>88</sup> studied the formation of 2-methylbenzimidazole from 2-nitrophenyl azide; this cyclization reaction was carried out under a N<sub>2</sub> atmosphere in alcoholic medium and under solar irradiation in the presence of TiO<sub>2</sub> Degussa P25. It is worth noting that the Authors have used different alcohols (methanol, ethanol, propanol and isopropanol) and the reaction yield and selectivity are sensitive to the alcohol used. A maximum yield of 93% after 4 h of reaction in an ethanolic medium was obtained. The reaction mechanism is reported in Fig. 20. Similarly for the formation of indazole from 2-nitrobenzyl azide, the azide is reduced to 2-nitrobenzylamine and then to diamine which undergoes cyclization leading to indazole as shown in Fig. 21.

The Authors report a further improvement in the conversion for the solar-mediated photocatalytic reaction by using Ag and Pt loaded TiO<sub>2</sub> Degussa P25.

The semiconductor photocatalysed addition of cyclopentene or cyclohexene to various novel electron-poor imines of type *p*-XC<sub>6</sub>H<sub>4</sub>(CN)C=N(COPh) (X = H, F, Cl, Br, Me, MeO) was investigated on cadmium sulfide photocatalyst.<sup>89</sup> Irradiation ( $\lambda > 350 \text{ nm}$ ) of silica supported cadmium sulfide surprisingly did not afford the expected olefin-imine adducts but an imine hydrocyanation product *via* an unprecedented dark reaction. However, when silica was replaced by zinc sulfide as the support, the expected homoallylic *N*-benzoyl- $\alpha$ -amino cyanides were isolated in yields of 65–84%. Thus,

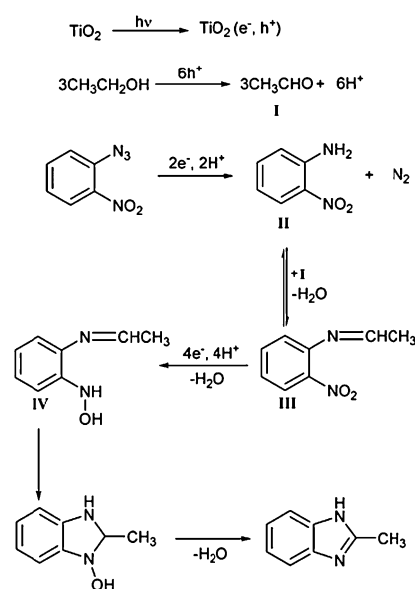


**Fig. 20** Formation of 2-methylbenzimidazole from 2-nitrophenyl azide in ethanol.<sup>88</sup>

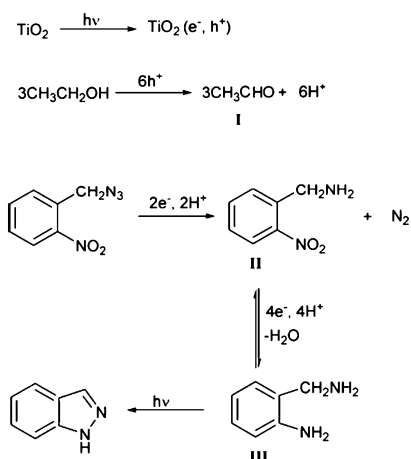


Fig. 21 Photocatalytic formation of indazole.<sup>88</sup>

chemoselectivity is introduced through replacing an insulating with a semiconducting support, a hitherto unknown effect in semiconductor photocatalysis. A tentative explanation provided by the Authors is related to the sign of the time resolved photovoltage. It was found that the CdS/ZnS interface increases the lifetime of photogenerated electron-hole pairs by about one order of magnitude as compared to the SiO<sub>2</sub>/CdS system. The reaction rate increases with increasing imine  $\sigma$ -Hammett constants and decreasing stability of intermediate benzyl radicals.<sup>89</sup>

### 3.4 Functionalization: C–C formation

The synthesis of organofluorine compounds has been carried out photocatalytically by using TiO<sub>2</sub>. The photogenerated electrons in the conduction band of the semiconductor reduce perfluoroalkyl iodide (the most common source for introducing perfluoroalkyl groups in organic molecules) to give perfluoroalkyl radical and iodide ion.<sup>90</sup> The radical species reacts with

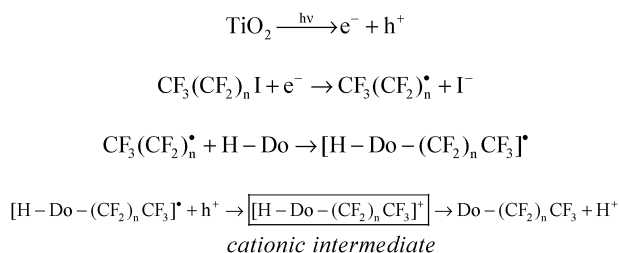


Fig. 22 Proposed mechanism for the synthesis of organofluorine compounds.<sup>90</sup>

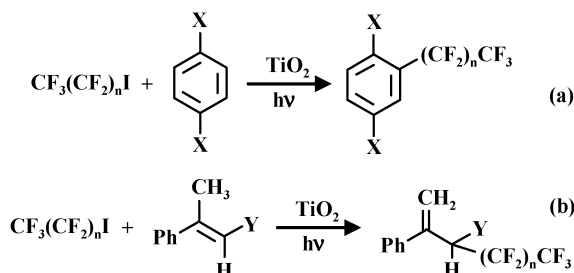


Fig. 23 Perfluoroalkylation of aromatic and aliphatic compounds.<sup>90</sup>

an organic molecule to give new radical species successively oxidized to the corresponding cationic intermediate, as reported in Fig. 22, where H-Do indicates an electron-rich compound:

In this way Iizuka *et al.*<sup>90</sup> have carried out the perfluoroalkylation of three aromatic rings (*p*-xylene, naphthalene and benzofuran) along with  $\alpha$ -methylstyrene and its related compounds 2-phenyl-2-butene and 3,4-dihydro-1-methylnaphthalene (Fig. 23):

## 4 Conclusions

This article summarizes some of the several recent investigations on selective organic transformations carried out by photocatalysis. Until a few years ago photocatalytic processes were considered to be only unselective. In these last years, however, photocatalysis is being demonstrated to be an alternative synthetic route in organic chemistry. The reacting systems here described are capable of carrying out selective oxidation and reduction processes that at proper reaction conditions may reach high conversions and yields. This is a very relevant result especially in the case of selective alcohol oxidation since it is quite difficult to avoid overoxidation of the formed aldehyde to the corresponding acid and other products.

Photocatalytic reactions do not use dangerous chemical reagents and solvents and they do not release harmful wastes into the environment. These significant advantages imply that photocatalysis may be an alternative “green” synthetic route.

In order to find wider application, photocatalytic processes need to be made faster and cheaper. In order to increase reaction rates, several studies devoted to elucidate the mechanistic details of photocatalytic reactions are essential and they are giving important information. As to concern the process economy, employment of sunlight is of course the ideal option even if solar photons need to be concentrated, especially in scaled up processes. Yet, mimicking Nature’s photosynthesis as a route to harness solar photons for use in conventional synthesis seems most promising. The Authors think that, when these two goals will be accomplished, rapid global spread of photocatalytic synthesis will take place.

## Notes and references

- (a) A. Fujishima and K. Honda, *Nature*, 1972, **238**, 37; (b) V. Augugliaro, V. Loddo, G. Palmisano, L. Palmisano and M. Pagliaro, *Clean by Light Irradiation. Practical Applications of Supported TiO<sub>2</sub>*, The Royal Society of Chemistry, Cambridge, 2010.
- (a) G. Palmisano, V. Augugliaro, M. Pagliaro and L. Palmisano, *Chem. Commun.*, 2007, 3425; (b) Y. Shiraishi and T. Hirai, *J. Photochem. Photobiol., C*, 2008, **9**, 157.
- H. Kominami, H. Sugahara and K. Hashimoto, *Catal. Commun.*, 2010, **11**, 426.
- M. Zhang, Q. Wang, C. Chen, L. Zhang, W. Ma and J. Zhao, *Angew. Chem., Int. Ed.*, 2009, **48**, 6081.
- Q. Wang, M. Zhang, C. Chen, W. Ma and J. Zhao, *Angew. Chem. Int. Ed.*, 2010, DOI: 10.1002/anie.201003621.
- A. Molinari, M. Bruni and A. Maldotti, *J. Adv. Ox. Tech.*, 2008, **11**, 143.
- A. Molinari, M. Montoncello, H. Rezala and A. Maldotti, *Photochem. Photobiol. Sci.*, 2009, **8**, 613.
- G. Marci, E. García-López, G. Mele, L. Palmisano, G. Dyrda and R. Słota, *Catal. Today*, 2009, **143**, 203.
- S. Higashimoto, N. Kitao, N. Yohida, T. Sakura, M. Azuma, H. Ohue and Y. Sakata, *J. Catal.*, 2009, **266**, 279.



- 10 C. Minero, G. Mariella, V. Maurino and E. Pelizzetti, *Langmuir*, 2000, **16**, 2632.
- 11 S. Kim and W. Choi, *J. Phys. Chem. B*, 2005, **109**, 5143.
- 12 (a) G. Palmisano, S. Yurdakal, V. Augugliaro, V. Loddo and L. Palmisano, *Adv. Synth. Catal.*, 2007, **349**, 964; (b) V. Loddo, S. Yurdakal, G. Palmisano, G. E. Imoberdorf, H. A. Irazoqui, O. M. Alfano, V. Augugliaro, H. Berber and L. Palmisano, *Int. J. Chem. React. Eng.*, 2007, **5**, A57.
- 13 (a) S. Yurdakal, G. Palmisano, V. Loddo, V. Augugliaro and L. Palmisano, *J. Am. Chem. Soc.*, 2008, **130**, 1568; (b) M. Addamo, V. Augugliaro, M. Bellardita, A. Di Paola, V. Loddo, G. Palmisano, L. Palmisano and S. Yurdakal, *Catal. Lett.*, 2008, **126**, 58.
- 14 (a) V. Augugliaro, T. Caronna, V. Loddo, G. Marci, G. Palmisano, L. Palmisano and S. Yurdakal, *Chem.-Eur. J.*, 2008, **14**, 4640; (b) S. Yurdakal, V. Loddo, G. Palmisano, V. Augugliaro, H. Berber and L. Palmisano, *Ind. Eng. Chem. Res.*, 2010, **49**, 6699.
- 15 S. Yurdakal, G. Palmisano, V. Loddo, O. Alagöz, V. Augugliaro and L. Palmisano, *Green Chem.*, 2009, **11**, 510.
- 16 N. Mizuno and M. Misono, *Chem. Rev.*, 1998, **98**, 199.
- 17 G. Marci, E. García-López, L. Palmisano, D. Carriazo, C. Martín and V. Rives, *Appl. Catal., B*, 2009, **90**, 497.
- 18 (a) S. Farhadi, M. Afshari, M. Maleki and Z. Babazadeh, *Tetrahedron Lett.*, 2005, **46**, 8483; (b) R. Wittenberg, M. A. Pradera and J. A. Navio, *Langmuir*, 1997, **13**, 2373.
- 19 H. Shen, H. Mao, L. Ying and Q. Xia, *J. Mol. Catal. A: Chem.*, 2007, **276**, 73.
- 20 S. Farhadi and M. Zaidi, *Appl. Catal., A*, 2009, **354**, 119.
- 21 (a) A. Maldotti, A. Molinari and F. Bigi, *J. Catal.*, 2008, **253**, 312; (b) J. A. Navio, M. Garcia Gomez, M. A. Pradera Adrian and J. Fuentes Mota, in *Studies in Surface Science and Catalysis*, ed. M. Guisnet, J. Barbier and J. Barrault, Elsevier, Amsterdam, 1993, vol. 78, p. 431.
- 22 P. Kluson, H. Luskova, L. Cervený, J. Klisakova and T. Cajtham, *J. Mol. Catal. A: Chem.*, 2005, **242**, 62.
- 23 J. Klisakova, P. Kluson and L. Cervený, *Collect. Czech. Chem. Commun.*, 2003, **68**, 1985.
- 24 A. Maldotti, A. Molinari and R. Amadelli, *Chem. Rev.*, 2002, **102**, 3811.
- 25 C. Murata, H. Yoshida, J. Kumagai and T. Hattori, *J. Phys. Chem. B*, 2003, **107**, 4364.
- 26 H. Yoshida, *Curr. Opin. Solid State Mater. Sci.*, 2003, **7**, 435.
- 27 H. Yoshida, M. G. Chaskar, Y. Kato and T. Hattori, *J. Photochem. Photobiol., A*, 2003, **160**, 47.
- 28 H. Yoshida, C. Murata and T. Hattori, *J. Catal.*, 2000, **194**, 364.
- 29 C. Murata, H. Yoshida and T. Hattori, *Chem. Commun.*, 2001, 2412.
- 30 P. Du, J. A. Moulijn and G. Mul, *J. Catal.*, 2006, **238**, 342.
- 31 R. Vinu and G. Madras, *Appl. Catal., A*, 2009, **366**, 130.
- 32 A. Maldotti, A. Molinari, R. Amadelli, E. Carbonell and H. García, *Photochem. Photobiol. Sci.*, 2008, **7**, 819.
- 33 M. Alvaro, C. Aprile, E. Benitez, E. Carbonell and H. García, *J. Phys. Chem. B*, 2006, **110**, 6661.
- 34 P. Ciambelli, D. Sannino, V. Palma, V. Vaiano, R. S. Mazzei, P. Eloy and E. M. Gaigneaux, *Catal. Today*, 2009, **141**, 367.
- 35 P. Ciambelli, D. Sannino, V. Palma, V. Vaiano and R. I. Bickley, *Appl. Catal., A*, 2008, **349**, 140.
- 36 B. Aurian-Blajeni, M. Halmann and J. Manassen, *Sol. Energy*, 1980, **25**, 165.
- 37 J. L. Ferry and W. H. Glaze, *Langmuir*, 1998, **14**, 3551.
- 38 O. V. Makarova, T. Rajh, M. C. Thurnauer, A. Martin, P. A. Kemme and D. Crokek, *Environ. Sci. Technol.*, 2000, **34**, 4797.
- 39 H. Tada, T. Ishida, A. Takao and S. Ito, *Langmuir*, 2004, **20**, 7898.
- 40 M. Shi and Y. M. Shen, *Curr. Org. Chem.*, 2003, **7**, 737.
- 41 T. Inoue, A. Fujishima, S. Konishi and K. Honda, *Nature*, 1979, **277**, 637.
- 42 Y. Shioya, K. Ikeue, M. Ogawa and M. Anpo, *Appl. Catal., A*, 2003, **254**, 251.
- 43 S. S. Tan, L. Zou and E. Hu, *Catal. Today*, 2006, **115**, 269.
- 44 X. V. Zhang, S. P. Ellery, C. M. Friend, H. D. Holland, F. M. Michel, M. A. A. Schoonen and S. T. Martin, *J. Photochem. Photobiol., A*, 2007, **185**, 301.
- 45 I. H. Tseng, J. C. S. Wu and H. Y. Chou, *J. Catal.*, 2004, **221**, 432.
- 46 W. Ling, C. Y. Jimmy, W. Xinchen, Z. Lizhi and Y. Jiaguo, *J. Solid State Chem.*, 2005, **178**, 321.
- 47 Y. Jiaguo, Y. Huogen, C. H. Ao, S. C. Lee, C. Y. Jimmy and H. Wingkei, *Thin Solid Films*, 2006, **496**, 273.
- 48 W. Ling, C. Y. Jimmy and F. Xianzhi, *J. Mol. Catal. A: Chem.*, 2006, **244**, 25.
- 49 Z. Sanbing, W. Jiankang, L. Haitao and W. Xiaolai, *Catal. Commun.*, 2008, **9**, 995.
- 50 C. C. Thiago, A. Jacqueline, S. P. F. Maria and G. Yoshitaka, *J. Electroanal. Chem.*, 2007, **609**, 61.
- 51 R. Seoudi, G. S. Elbahy and Z. A. E. Sayed, *Opt. Mater.*, 2006, **29**, 304.
- 52 G. A. Kumar, J. Thomas and N. V. Unnikrishnan, *J. Mater. Sci.*, 2000, **35**, 2539.
- 53 G. Raed, *Spectrochim. Acta, Part A*, 2009, **72**, 455.
- 54 L. Shaohua, Z. Zhihuan and W. Zhizhong, *Photochem. Photobiol. Sci.*, 2007, **6**, 695.
- 55 Z. Zhao, J. Fan and Z. Wang, *J. Clean. Prod.*, 2007, **15**, 1894.
- 56 Z. Zhao, J. Fan, M. Xie and Z. Wang, *J. Clean. Prod.*, 2009, **17**, 1025.
- 57 O. Ozcan, F. Yukruk, E. U. Akkaya and D. Uner, *Top. Catal.*, 2007, **44**, 523.
- 58 O. Ozcan, F. Yukruk, E. U. Akkaya and D. Uner, *Appl. Catal., B*, 2007, **71**, 291.
- 59 T. Nguyen, J. C. S. Wu and C. Chiou, *Catal. Commun.*, 2008, **9**, 2073.
- 60 R. E. Marinangeli and D. F. Ollis, *AIChE J.*, 1977, **23**, 415.
- 61 R. E. Marinangeli and D. F. Ollis, *AIChE J.*, 1980, **26**, 1000.
- 62 P. Pan and Y. Chen, *Catal. Commun.*, 2007, **8**, 1546.
- 63 Y. Liu, B. Huang, Y. Dai, X. Zhang, X. Qin, M. Jiang and M. Whangbo, *Catal. Commun.*, 2009, **11**, 210.
- 64 A. Kudo, K. Omori and H. Kato, *J. Am. Chem. Soc.*, 1999, **121**, 11459.
- 65 M. Oshikiri and M. Boero, *J. Phys. Chem. B*, 2006, **110**, 9188.
- 66 T. Nguyen and J. C. S. Wu, *Appl. Catal., A*, 2008, **335**, 112.
- 67 F. Zhang, R. L. Jin, J. X. Chen, C. Shao, W. L. Gao, L. Li and N. J. Guan, *J. Catal.*, 2005, **232**, 424.
- 68 S. Rengaraj and X. Z. Li, *Chemosphere*, 2007, **66**, 930.
- 69 S. Sanuki, T. Kojima, K. Arai, S. Nagaoka and H. Majima, *Metall. Mater. Trans. B*, 1999, **30**, 15.
- 70 T. Mori, J. Suzuki, K. Fujimoto, M. Watanabe and Y. Hasegawa, *J. Sol-Gel Sci. Technol.*, 2000, **19**, 505.
- 71 A. Bystrom and A. M. Bystrom, *Acta Crystallogr.*, 1950, **3**, 146.
- 72 Y. Fujiki, S. Takenouchi, Y. Onoda, M. Watanabe, S. Yoshikado, T. Ohachi and I. Taniguchi, *Solid State Ionics*, 1987, **25**, 131.
- 73 S. O. Flores, O. Rios-Bernij, M. A. Valenzuela, I. Córdova, R. Gómez and R. Gutiérrez, *Top. Catal.*, 2007, **44**, 507.
- 74 A. Maldotti, L. Andreotti, A. Molinari, S. Tollari, A. Penoni and S. Cenini, *J. Photochem. Photobiol., A*, 2000, **133**, 129.
- 75 V. Brezova, P. Tarabek, D. Dvoranova, A. Stasko and S. Biskupic, *J. Photochem. Photobiol., A*, 2003, **155**, 179.
- 76 H. Kominami, S. Iwasaki, T. Maeda, K. Imamura, K. Hashimoto, Y. Kera and B. Ohtani, *Chem. Lett.*, 2009, **38**, 410.
- 77 J. S. D. Kumar, M. H. Mankit and T. Toyokuni, *Tetrahedron Lett.*, 2001, **42**, 5601.
- 78 Y. Moglie, C. Vitale and G. Radivoy, *Tetrahedron Lett.*, 2008, **49**, 1828.
- 79 M. Sathish, B. Viswanathan and R. P. Viswanath, *Appl. Catal., B*, 2007, **74**, 307.
- 80 T. C. Jagadale, S. P. Takale, R. S. Sonawane, H. M. Joshi, S. I. Patil, B. B. Kale and S. B. Ogale, *J. Phys. Chem. C*, 2008, **112**, 14595.
- 81 H. Wang, J. Yan, W. Chang and Z. Zhang, *Catal. Commun.*, 2009, **10**, 989.
- 82 D. Astruc, *New J. Chem.*, 2005, **29**, 42.
- 83 Y. Inaki, H. Yoshida and T. Hattori, *J. Phys. Chem. B*, 2002, **106**, 9098.
- 84 T. Tanaka, S. Matsuo, T. M. Kaeda, H. Yoshida, T. Funabiki and S. Yoshida, *Appl. Surf. Sci.*, 1997, **121–122**, 296.
- 85 H. Yoshida, N. Matsushita, Y. Kato and T. Hattori, *Phys. Chem. Chem. Phys.*, 2002, **4**, 2459.
- 86 H. Yoshida, N. Matsushita, Y. Kato and T. Hattori, *J. Phys. Chem. B*, 2003, **107**, 8355.
- 87 Y. Kato, H. Yoshida and T. Hattori, *Microporous Mesoporous Mater.*, 2002, **51**, 223.
- 88 K. Selvam, B. Krishnakumar, R. Velmurugan and M. Swaminathan, *Catal. Commun.*, 2009, **11**, 280.
- 89 M. Gartner, J. Ballmann, C. Damm, F. K. Heinemann and H. Kisch, *Photochem. Photobiol. Sci.*, 2007, **6**, 159.
- 90 M. Iizuka and M. Yoshida, *J. Fluorine Chem.*, 2009, **130**, 926.